Micro-milling of Spent Granular Activated Carbon for its Possible Reuse as an Adsorbent: Remaining Capacity and Characteristics

Long Pan [a], Yuichi Takagi [a], Yoshihiko Matsui [b*], Taku Matsushita [b], Nobutaka Shirasaki [b]

a Graduate School of Engineering, Hokkaido University, N13W8, Sapporo 060-8628, Japan

b Faculty of Engineering, Hokkaido University, N13W8, Sapporo 060-8628, Japan

* Corresponding author. Tel./fax: +81-11-706-7280

E-mail address: matsui@eng.hokudai.ac.jp

Abstract

We milled granular activated carbons (GACs) that had been used for 0–9 years in water treatment plants and produced carbon particles with different sizes and ages: powdered activated carbons (PAC, median diameter 12–42 μm), superfine PAC (SPAC, 0.9–3.5 μm), and submicron-sized SPAC (SSPAC, 220–290 nm). The fact that SPAC produced from 1-year-old GAC and SSPAC from 2-year-old GAC removed 2-methylisoborneol (MIB) from water with an efficiency similar to that of virgin PAC after a carbon contact time of 30 minutes suggests that spent GAC could be reused for water treatment after being milled. This potential for reuse was created by increasing the equilibrium adsorption capacity via reduction of the carbon particle size and improving the adsorption kinetics. During long-term (>1 year) use in GAC beds, the volume of pores in the carbon, particularly pores with widths of 0.6–0.9 nm, was greatly reduced. The equilibrium adsorption capacities of the carbon for compounds with molecular sizes in this range could therefore decrease with increasing carbon age. Among these compounds, the decreases of capacities were prominent for hydrophobic compounds, including MIB. For hydrophobic compounds, however, the equilibrium adsorption capacities could be increased with decreasing carbon particle size. The iodine number, among other indices, was best correlated with the equilibrium adsorption capacity of the MIB and would be a good index to assess the remaining MIB adsorption capacity of spent carbon. Spent GAC can possibly be reused as SPAC or SSPAC if its iodine number is ≥600 mg/g.

Keywords: 2-methylisoborneol, iodine number, SPAC, used carbon

1. Introduction

Adsorption by granular activated carbon (GAC) is widely used in drinking water treatment to remove disinfection byproduct precursors (DBPPs), natural organic matter (NOM), and organic micro-pollutants (OMPs); GAC adsorption also serves as a barrier, inter alia, to occasional spikes of toxic substances in source waters (Corwin et al., 2012; Matsui et al., 2002b; Owen, 1998; Paune et al., 1998). Because of the limited adsorption capacity of GAC, however, removal of these compounds requires that the GAC be replaced from time to time. Otherwise, removal efficiencies deteriorate with time as the GAC filtration operation progresses. Before the breakthrough of a target adsorbate, the GAC needs to be replaced if the removal ability of the adsorbate is to be maintained. Normally, the spent GAC goes through a regeneration process because it is more cost effective to regenerate spent GAC than to purchase virgin GAC (Lambert et al., 2002; Sontheimer et al., 1988). Spent GAC is sometimes replaced with virgin GAC, for example, when the cost of virgin GAC at the market is similar to or somewhat higher than the cost of regeneration (Iwamoto et al., 2014).

In the regeneration process, adsorption sites on the GAC are refreshed by desorption, decomposition, or degradation of the adsorbates loaded on the GAC. Although regeneration restores the adsorption capacity of the GAC to an extent that depends on the regeneration process employed, there are many disadvantages to regeneration. Those disadvantages include 1) for thermal regeneration, high energy demand, loss of GAC itself, accumulation of metals in the GAC, and the high pH of water initially treated by the regenerated GAC (Lambert et al., 2002; San Miguel et al., 2001); 2) for chemical regeneration, the requirement

for additional treatment to deal with the regenerants, such as organic solvents, that remain in the regenerated GAC, and the formation of by-products during regeneration (Alvarez et al., 2004; Lim et al., 2005; Martin et al., 1985); 3) for biological regeneration, the long reaction time required for regeneration and the failure of adsorption sites loaded with non-biodegradable adsorbates to recover (Nakano et al., 2000; Scholz et al., 1998). There is hence a need for an alternative option to use spent GAC without regeneration.

As mentioned above, the frequency of GAC replacement is determined by the breakthrough behavior of target compounds. In water treatment plants, where multiple adsorbates are targeted for removal, the frequency of GAC replacement is determined by the earliest breakthrough of the multiple target adsorbates. Previous research has shown that NOM and DBPPs break through GAC adsorbers earlier than OMPs when these compounds coexist as mixtures in water (Kennedy et al., 2015; Summers et al., 2013). Thus, the adsorption capacities may still remain for OMPs even when the GAC has been replaced as a result of the breakthrough of NOMs and/or DBPPs.

The adsorption capacity that remains in spent GAC is likely to be low compared with the capacity of virgin and regenerated GAC. However, the disadvantage of low capacity can be compensated for if the adsorptive kinetics of the carbon is high. When spent GAC is milled into small-size particles, the increase of the exterior specific surface area leads to high adsorption kinetics that enhance the uptake rate of adsorbates. Extremely high adsorption kinetics has been reported for superfine powdered activated carbon (SPAC) with a particle diameter $\cong$1 μm; SPAC is produced by the micro-milling of virgin powdered activated carbon (Bonvin et al., 2016; Matsui et al., 2004; Matsui et al., 2013a).

Particle size reduction, moreover, can be expected to enhance adsorption capacities as well as adsorption kinetics (Bonvin et al., 2016; Hu et al., 2015; Knappe et al., 1999; Matsui et al., 2010). Enhancement of adsorption capacity may be mandatory for reuse of spent GAC because even very high kinetics cannot compensate for the disadvantage of inadequate capacity.

The objective of this research was to investigate the production of PAC, SPAC, and submicron-sized SPAC from spent GAC and the application of these as adsorbents to remove OMPs, in particular, 2-methylisoborneol (MIB), which is a conventional target OMP due to its association with an unpleasant earthy/musty taste and odor, which impair the palatability of drinking water (Cook et al., 2001; Newcombe et al., 1997). Changes of equilibrium adsorption capacities and adsorptive removal rates with carbon particle size and carbon age are discussed in conjunction with the metrics of standard indicators of activated carbon characteristics.

2. Materials and methods

2.1 *Activated carbon*

GACs were collected from GAC beds of drinking water treatment plants operated by the Bureau of Waterworks of the Tokyo Metropolitan Government, the Public Enterprise Bureau of Ibaraki Prefectural Government, and the Ishikari-Seibu Water Supply Authority (Table 1). After being thoroughly mixed, each GAC was separated into several portions and kept under

a moist condition at 4 °C in a refrigerator. Some portions were sterilized by autoclaving or gamma ray irradiation, which are described in detail in section S1 of the Supplementary Information (SI). Unless specified, the sterilized samples discussed in this paper refer to the samples autoclaved at 63 °C for 30 min.

The GACs were pulverized into fine particles of three particle-size categories according to their median diameter (D50): powdered activated carbon (PAC, D50: 12–42 μm), superfine PAC (SPAC, D50: 0.9–3.5 μm), and submicron-sized SPAC (SSPAC, D50: 0.22–0.29 μm). The GACs had D50s of 1.5–2.3 mm. The details of the pulverization process and the particle size distributions of all carbon samples are described in the SI (section S2 and Fig. S6). Tables S1–S3 of the SI list all activated carbon samples and related experimental applications. These samples were given unique three-term designations as follows. The first term indicates the name of the water treatment plant where the GAC was collected and the number of years the GAC was used (note: zero "0" year indicates virgin carbon). The second term indicates the method of pretreatment of the GAC. An "n" indicates "no pretreatment", "a" indicates "autoclave pretreatment", and "g" indicates "gamma irradiation pretreatment". The final term indicates the particle size category of the carbon: GAC, PAC, SPAC, and SSPAC. KM2-a-SPAC, for example, means SPAC produced by milling from autoclaved GAC, which was sampled at the Kanamachi Water Treatment Plant after being used for 2 years. The carbons produced from the GACs given no pretreatment were used for adsorption experiments with carbon-water contact times < one day. Those produced from the GACs pretreated by autoclaving were used for adsorption experiments with carbon-water contact times > one day to avoid any biodegradation effect. Autoclaving did not substantially

132 influence the equilibrium adsorption capacity (e.g. sections S1.2 and S1.3 of the SI). The
133 PAC, SPAC, and SSPAC samples were stored in ultrapure water in the form of slurries at
134 4 °C after vacuum conditioning for 20 min to remove any air from the activated carbon pores.
135 The pore size distributions of the activated carbons were obtained by using the nitrogen
136 gas adsorption-desorption method (Autosorb-iQ, Quantachrome Instruments, Kanagawa,
137 Japan). The isotherm data for nitrogen gas at 77.4 K was analyzed by (1) the Barrett-Joyner-
138 Halenda (BJH) method for the mesopore region (pore width >2 nm) and (2) the quench solid
139 density functional theory (QSDFT) for the micropore region (pore width = 0.6–2 nm)
140 (ASiQwin, ver.3.01, Quantachrome Instruments). Iodine, phenol, methylene blue (MB), and
141 sodium liner-dodecylbenzene sulfonates (hereafter ABS) numbers were measured according
142 to the standard methods of the Japan Water Works Association (K 113:2005-2) (JWWA,
143 2005). The details of the measurement methods are described in section S3 of the SI.
144
145 2.2 *Adsorbates*
146
147 MIB was the main target compound in this study. Reagent MIB was dissolved in natural
148 water (the raw water entering the Kanamachi Water Purification Plant, the same plant where
149 the main target GACs were collected) or in organic-free ionic water that was made from
150 ultrapure water by adding ions at concentrations identical to their concentrations in the
151 natural water (details are provided in section S4 of the SI). The concentrations of MIB were
152 measured by using deuterium-labeled geosmin (geosmin-d3) as an internal standard in a
153 purge-and-trap concentrator (P&T) coupled to a gas chromatograph-mass spectrometer

154 (GC/MS); the *m/z* 95 peak was assumed to correspond to MIB and the *m/z* 115 peak to
155 geosmin-d3. Two P&T-GC/MS systems were used: (1) a Model 4660 Eclipse (Kinryo
156 Electric Co., LTD, Osaka, Japan) coupled with an Agilent 7890A/5975MSD (Agilent
157 Technologies, Inc., CA, USA); and (2) an Aqua PT 5000 J (GL Sciences, Inc., Tokyo, Japan)
158 coupled with a GCMS-QP2010 Plus (Shimadzu Co., Kyoto, Japan).
159 In addition to MIB, some compounds with environmental relevancy and compounds used
160 for adsorbability indices were tested as supplementary adsorbates: geosmin, iodine, phenol,
161 acetaminophen, MB, ABS, poly(styrenesulfonic acid) sodium salt with an average molecular
162 weight (MW) of 210 (PSS-210), and PSS-6400 with average MW 6400. These compounds
163 were selected to cover a variety of hydrophobicities and molecular sizes. Section S5 of the
164 SI provides details of the anaytical methods used to quantify these compounds. Except for
165 PSS-210 and PSS-6400, which were purchased from Sigma-Aldrich Co. LLC. (St. Louis,
166 Missouri, USA), all of these chemical reagents were purchased from Wako Pure Chemical
167 Industries, Ltd., (Osaka, Japan).
168
169 2.3 *Batch adsorption tests*
170
171 In all adsorption kinetics and equilibrium tests, specified amounts of carbon were added to
172 vials containing either 100 or 110 mL of a solution of the target compound, and the vials were
173 manually shaken and then agitated on a mechanical shaker for a pre-determined period of
174 time at a constant temperature of 20 °C in the dark. The carbon-solution contact time ranged
175 from 10 minutes to 24 hours for the MIB adsorption kinetics tests; it was set to 1–2 weeks

for the MIB adsorption equilibrium tests. After the pre-determined carbon-solution contact time, the carbon-solution suspension were each filtered through a 0.2-μm membrane filter (DISMIC-25HP; Toyo Roshi Kaisha, Ltd., Tokyo, Japan, SSPAC-solution suspension was filtered twice) to separate carbon, and the concentrations of the adsorbate in the filtrates were then measured. Solid-phase concentrations of adsorbates were calculated from mass balances. Section S4 of the SI provides details of the experimental methods, including experiments with other compounds.

3. Results and discussion

3.1 *MIB adsorption kinetics*

We tested KM0, KM1, KM2, and KM3 after having determined that four-year old carbons including their PACs and SPACs had no adsorptive removal ability (section S1 of the SI). Fig. 1 shows the time-course changes of normalized MIB concentrations in the adsorption kinetic tests. Fig. 1a shows the results of KM0 (virgin GAC and the PAC and the SPAC produced from it). There were clear increases of MIB removal rates with decreasing particle size when the GAC was milled to PAC and SPAC. The MIB removal rate was higher for SPAC than PAC, as reported elsewhere (Matsui et al., 2007; Matsui et al., 2013a; Pan et al., 2016). Improvements of MIB removal rates with decreasing carbon size were also observed for 1-to-3-year-old spent carbons (Fig. 1b,c,d).

197 To further clarify the MIB removal efficiencies of spent carbons, we performed
198 adsorption experiments with varying dosages and a fixed carbon-water contact time of 30
199 min, a time that is often used in actual water purification treatments. Fig. 2 shows the results.
200 The SPAC and SSPAC produced from one-year-old carbons (KM1-n-SPAC) achieved the
201 same removal rate as virgin PAC (KM0-n-PAC), a removal rate that might be regarded as a
202 feasible goal from a practical standpoint. In the two-year-old carbon series, SPAC did not
203 achieve the same reduction rate as the virgin PAC, but SSPAC did. None of the three-year-
204 old carbons, including its SSPAC, achieved the same removal rate as the virgin PAC (KM0-
205 n-PAC).
206
207 3.2 *MIB adsorption capacity*
208
209 As described in section 3.1, the one-year-old and two-year-old carbons, when milled to
210 micron- and submicron-diameter particles, respectively, were similar to the virgin PAC in
211 terms of MIB removal ability. However, the uptake rate of MIB by carbon with ages ≥3 years
212 was less than that of virgin PAC, even if the particle sizes were decreased to enhance the
213 uptake rate of MIB. Because sufficient adsorbate uptake cannot be expected when the carbon
214 does not have a certain level of equilibrium adsorption capacity, we examined the equilibrium
215 adsorption capacities of the spent carbons. Fig. S7 in the SI shows the adsorption isotherms
216 of the 32 carbons. The equilibrium MIB adsorption capacities decreased with increasing
217 carbon age and increased as the particle size decreased.
218 To clarify these trends, the equilibrium adsorption capacities of carbon with different

ages were plotted against the carbon particle sizes. Equilibrium adsorption capacities were quantified in terms of the Freundlich capacity parameter in the unit of $(ng/mg)(L/100\ ng)^{1/n}$, which is equivalent to the solid-phase concentration in equilibrium with a liquid-phase concentration of 100 ng/L after fitting the isotherm data to the Freundlich model. A reduction of the MIB adsorption capacities with carbon age was clearly apparent (Fig. 3). The longer the carbon aged, the lower the MIB adsorption capacity of the carbon. A similar phenomenon has previously been observed for adsorption of a pesticide (atrazine) onto PAC, which was used for a few months in an immersed microfiltration membrane system (Lebeau et al., 1999). Equilibrium adsorption capacities in our study also increased with decreasing carbon particle size. A similar phenomenon has been reported for virgin PAC and its SPAC (Matsui et al., 2010; Matsui et al., 2012) as well as for one-year-old used GAC and its PAC (Hu et al., 2015; Knappe et al., 1999).

Among the spent carbons up to three years old, the oldest carbon (KM3-a series) showed the most dramatic increase of adsorption capacity: the adsorption capacity increased 6.8-fold when the carbon diameter decreased from 22 μm to 200 nm. Adsorption capacity increased 12-fold when the diameter of two-year-old carbon decreased from 1.9 mm to 250 nm. Finally, the capacity of SSPAC produced from two-year-old GAC was similar to that of virgin GAC. Adsorption capacities decreased with increasing age of carbons, but they increased as the particle size decreased. As described in section 3.1, when spent GAC was milled to micron- and submicron-size particles, its ability to remove MIB at a given contact time was enhanced, and the adsorption capability of the carbon was similar to that of virgin PAC. This enhancement can be explained by the faster adsorbate uptake rate due to the broadening of

241 the outer surface area (carbon-water contact area) and reduction of the intra-particle diffusion
242 path length. The results presented in this section clearly reveal that the enhancement of MIB
243 removal efficiency was due to both an increase of equilibrium adsorption capacity and an
244 increase of adsorbate uptake rate.
245
246 3.3 *Pore size distributions*
247
248 The pore size distribution of activated carbon particles is an important parameter related to
249 their equilibrium adsorption capacity. It has been reported previously that the change in
250 carbon particle size by micro-milling does not result in any substantial change in pore size
251 distribution (Ando et al., 2010; Matsui et al., 2015). The results of our study also confirmed
252 that the pore size distributions were similar for different-size particles (PAC, SPAC, and
253 SSPAC) with the same age, although experimental errors were apparent in the data for one-
254 year-old carbon (Fig. S8 of the SI). We therefore considered the effect of carbon age on pore
255 size distribution after averaging data for carbons of the same age.
256 Between carbons of different ages, clear differences were apparent in the distribution of
257 small-size micropores (pores with widths 0.6–0.9 nm) (Fig. 4). In contrast, no large
258 difference was apparent in the distribution of pores with widths >0.9 nm, including
259 mesopores (Fig. 4 and Fig. S9 of the SI). The volume of the small-size micropores decreased
260 from 0 to 3 years, in particular during the first year, whereas the volume of the larger-size
261 pores did not decrease largely [the decreases were also seen for the BET (Brunauer-Emmett-
262 Teller) surface areas as shown in Table S6 of the SI]. If loading of NOM on carbon is the

main cause of carbon fouling, this result is intriguing, because NOM is believed to adsorb mainly onto mesopores rather than micropores (Li et al., 2002b; Li et al., 2003; Newcombe et al., 2002a). A previous study of four-year-old used GAC (Kameya et al., 1997), however, has revealed a similar phenomenon, namely that micropore volume decreases to a larger extent than mesopore volume, and it decreases rapidly at the beginning of an operation of a GAC bed. A change of the volume of micropores could be caused by accumulation of synthetic organic micro-pollutants as well as low-MW NOM present in the raw waters because the effluents from wastewater treatment plants are discharged into the upstream of the river.

In our experiment, the rapid drop of micropore volume after one year was concomitant with the decrease of MIB adsorption capacity: the adsorption capacity dropped relatively rapidly during the first year and declined more slowly afterward (Fig. 3, note that the ordinate is at log scale). The similarity between the trends of micropore volume and MIB adsorption capacity is in accord with the common understanding that MIB is mainly adsorbed in micropores (Greenwald et al., 2015; Newcombe et al., 1997; Quinlivan et al., 2005; Yu et al., 2007).

3.4 *Iodine, phenol, MB, and ABS numbers*

The amounts of iodine, phenol, MB, and ABS adsorbed under specified conditions are called the iodine, phenol, MB, and ABS numbers, respectively. These numbers were used as metrics of the adsorptive removal ability of activated carbons. Fig. 5 shows the changes of these

285 numbers for carbons of different ages against carbon particle size calculated from the data in
286 Fig. S10 of the SI.

287 For both the iodine number and phenol number (Figs. 5a and b, respectively),
288 dependencies on carbon age were clearly apparent: the older spent carbons adsorbed smaller
289 amounts of iodine and phenol. The dependencies on carbon age were small for the MB
290 number (Fig. 5c). For the ABS number (Fig. 5d), the dependence on carbon age was also
291 small at a carbon particle diameter of about 0.2 μm, but it was large at a carbon particle
292 diameter greater than a few microns. With respect to dependence on carbon particle size,
293 iodine numbers increased slightly with decreasing particle size. In the case of the phenol
294 number, no increase and even slight decreases were observed when the size of the carbon
295 particles was reduced. In the case of the MB and ABS numbers (Figs. 5c and d, respectively),
296 a dependency on carbon particle size was clearly apparent. Among the four index numbers
297 of the KM carbon series, the iodine number showed the highest correlation (R^2 = 0.97) with
298 the MIB adsorption capacity (Fig. S11a of the SI). The MIB adsorption capacity increased
299 with increasing iodine number, even when the data came from carbons with the same age.
300 Such a trend was not apparent for phenol, for which the correlation was second highest
301 among the four indices (R^2 = 0.83). The correlation for iodine was high (R^2 = 0.88), even
302 when the data included carbons from different materials and carbons used in different
303 treatment plants that treated different waters (Fig. 6). However, deviations from the
304 regression line were somewhat large for some carbons that had been used in the other water
305 treatment plants (KS0.1 and IS4). The followings are considered as the reasons why iodine
306 showed the highest correlation: 1) its molecular size, which is not largely different from that

of MIB, 2) fast adsorption kinetics of iodine so that iodine number, which was obtained in the contact time of 15 min, would nearly be iodine adsorption capacity at equilibrium (e.g. on the other hand, phenol number was not equilibrium capacity), and 3) among the four indices, iodine could be hydrophobic as is MIB (Figure 7).

Overall, the iodine number was a good index for roughly estimating the remaining MIB adsorption capacity of the spent carbons. The MIB removal ability of SSPAC produced from two-year-old GACs was similar to that of virgin PAC, as described in the section 3.1, and the iodine numbers of the two-year-old carbons were about 600 mg/g (Fig. 6). Therefore, if spent carbon still has an iodine number > 600 mg/g, it could be reused as SSPAC (or possibly as SPAC), regardless of the raw material that was the source of the carbon and the history of carbon use.

3.5 *Influence of adsorbate properties on adsorption capacity*

Among the four indices, the iodine number (Fig. 6) was most highly correlated with MIB adsorption capacity (section 3.4). This correlation reflects the large degree of the adsorption capacity dependence on carbon age and to a certain degree its dependence on carbon size (Fig. 5a). To determine which properties of the adsorbates led to the adsorption capacity dependencies on carbon particle size and carbon age, we measured the adsorption isotherms of a variety of compounds on PAC, SPAC, and SSPAC that were produced from two-year-old used GAC (KM2-GAC) and virgin GAC (KM0-GAC). The adsorption capacity of each carbon sample for each adsorbate was calculated from the corresponding adsorption isotherm

329 at equilibrium (Fig. S12 of the SI). The calculation was carried out using the same procedure
330 explained in section 3.2 for the MIB adsorption capacity. To avoid the effect of background
331 adsorptive substances (including NOMs) in natural water, especially for adsorption onto
332 virgin carbons, all the adsorption experiments were conducted in organic-free water, the ionic
333 composition of which was the same as that of the natural water. For MIB and geosmin, the
334 adsorption capacities were calculated at equilibrium with a liquid-phase concentration of 100
335 ng/L. For phenol, acetaminophen, PSS-210, iodine, MB, ABS, and PSS-6400, half of the
336 initial concentrations was used as an equilibrium liquid-phase concentration to calculate the
337 adsorption capacity (data for lower concentrations were not obtainable because of analytical
338 errors). The degree of the capacity dependence on carbon age was then quantified from the
339 ratio of the adsorption capacities of virgin SPAC and spent SPAC. This ratio is hereafter
340 called the age-dependency index. The degree of the capacity dependence on carbon particle
341 size was quantified in terms of the slopes of log-log plots of capacities vs. carbon particle
342 diameters (Matsui et al., 2012). This slope is hereafter called the size-dependency index.

343 Among the several properties of the adsorbates that could possibly have influenced the
344 adsorption capacities of the spent carbon, we first focused on molecular size, because changes
345 were observed in the volume of the small-size micropores as the carbon aged (section 3.3).
346 As a metric of molecular size, we used the minimal projection diameter (MPD) because it is
347 the property that decides which carbon pores are available for the adsorbate molecule
348 (Kasaoka et al., 1989; Li et al., 2002a; Pelekani et al., 2000; Sontheimer et al., 1988). MPDs
349 were calculated from the three-dimensional structures of molecules predicted by using
350 Marvin Sketch (v.16.5.16.0, ChemAxon Ltd, Hungary).

351 The age-dependency and size-dependency indices of the nine compounds are plotted
352 against their MPDs in Figs. 7 and 8, respectively. The age dependencies of ABS and PSS-
353 6400 were low, perhaps because of their large sizes. Because pores with widths >0.9 nm did
354 not change much with age (section 3.3), ABS and PSS-6400, which have MPDs of 1.22 nm
355 and 2.52 nm, respectively, would not have been influenced from loading of (probably) NOM
356 during the GAC operation. Among the compounds with MPDs of 0.6–0.9 nm, MIB and
357 geosmin exhibited high age dependency. MIB and geosmin are hydrophobic compounds with
358 high log-Kow values of 3.31 and 3.57, respectively, and they adsorb on hydrophobic basal
359 plane sites (Ahnert et al., 2003; Considine et al., 2001; Moreno-Castilla, 2004). Hydrophilic
360 compounds such as acetaminophen, which adsorb on specific sites as well as basal planes
361 (Rey-Mafull et al., 2014), exhibited small age-dependency, which is in accord with a previous
362 study that suggests a small effect from the loading of background matrix on acetaminophen
363 adsorption (Coimbra et al., 2015).
364 It has therefore been suggested that the hydrophobic basal plane sites contained in the
365 pores (0.6–0.9 nm) were probably intensively occupied by hydrophobic compounds during
366 the long-term operation of the GAC. These hydrophobic compounds would be low-MW
367 NOM (Kilduff et al., 1998; Newcombe et al., 1997; Newcombe et al., 2002b). Although low-
368 MW NOMs might be overall more hydrophilic than hydrophobic (Aiken et al., 1992; Croué,
369 2004; Velten et al., 2011), hydrophobic fractions of low-MW NOMs with a benzene moiety,
370 phenolic structures, and conjugated double bonds (Świetlik et al., 2004), which would
371 promote hydrophobic interactions, would occupy the hydrophobic sites in the micropores
372 and thus reduce the capacities of MIB and similar compounds to adsorb (Matsui et al., 2002a;

373 Schmit et al., 2002; Zietzschmann et al., 2016). Hydrophobic synthetic organic micro-
374 pollutants, which would be present in waters treated by the GACs, would also occupy
375 hydrophobic adsorption sites in the micropores and thereby reduce the adsorption capacities
376 of MIB and similar compounds. Overall, this research suggests that age dependency results
377 from micropores and adsorbates with molecular diameters of 0.6–0.9 nm and high
378 hydrophobicity.

379 Of relevance to the carbon-size-dependency is the fact that early researchers discovered
380 that some hydrophobic organic micro-pollutants and high-MW compounds were adsorbed
381 mainly on the exterior of carbon particles due to their limited penetration distances (Matsui
382 et al., 2013a; Matsui et al., 2014). The capacity of MIB, geosmin, and humic substances to
383 adsorb onto GAC and PAC would thus increase when the GAC/PAC particle was milled to
384 a smaller size (Amaral et al., 2016; Ando et al., 2010; Bonvin et al., 2016; Knappe et al.,
385 1999; Matsui et al., 2015; Matsui et al., 2013b). The high dependencies on carbon particle
386 size of the capacities of MIB, geosmin, PSS-6400, and ABS to adsorb onto spent carbons
387 (Fig. 8) are in line with this previous finding, which was reported for virgin carbons.
388 Similarly, for large molecular-size compounds and hydrophobic compounds with even small
389 molecular sizes, the equilibrium adsorption capacities on spent as well as virgin carbons
390 would increase when carbon particle size was decreased by milling.

391

392 **4. Conclusions**

393

(1) Equilibrium MIB adsorption capacities of GACs used in water treatment plants for 1–3 years increased when the GACs were milled to PAC, SPAC, and SSPAC, which are characterized by progressively smaller particle sizes.

(2) By milling the GACs used in water purification plants for 1–2 years, it is possible to reuse them as SPAC or SSPAC adsorbents to remove MIB. This reusability reflects the increased adsorption capacity and higher adsorptive kinetics of smaller particles.

(3) The MIB adsorption capacity of spent carbons was well correlated with iodine numbers. Therefore, iodine number could be a metric of remaining MIB adsorption capacity.

(4) During the three years of GAC use, the volume of the micropores with widths of 0.6–0.9 nm was greatly reduced compared with that of pores with larger widths.

(5) The adsorption capacity of spent carbon for hydrophobic compounds with MPDs of 0.6–0.9 nm, including MIB, depended on carbon age; the capacity decreased greatly with carbon age.

(6) The adsorption capacity of spent carbon for compounds with large MPDs and/or high hydrophobicities depended on the carbon particle size; the capacity increased with decreasing particle size.

Acknowledgments

We thank the Bureau of Waterworks of the Tokyo Metropolitan Government, the Public Enterprise Bureau of Ibaraki Prefectural Government, and the Ishikari-Seibu Water Supply

Authority for providing GAC samples. Thanks are also due to Mr. Koudai Sekiguchi and Ms. Aki Yamamoto for their experimental helps. This study was supported by a Grant-in-Aid for Scientific Research S (24226012 and 16H06362) from the Japan Society for the Promotion of Science and was partly supported by a Health and Labour Sciences Research Grant (Research on Health Security Control) from the Ministry of Health, Labour, and Welfare, Japan. We acknowledge the financial support in the form of a scholarship (201306460006) from the China Scholarship Council (CSC) to Long Pan for his doctoral research.

References

Ahnert, F., Arafat, H.A. and Pinto, N.G., 2003. A Study of the Influence of Hydrophobicity of Activated Carbon on the Adsorption Equilibrium of Aromatics in Non-Aqueous Media. Adsorption 9(4), 311-319.

Aiken, G.R., McKnight, D.M., Thorn, K.A. and Thurman, E.M., 1992. Isolation of hydrophilic organic acids from water using nonionic macroporous resins. Organic Geochemistry 18(4), 567-573.

Alvarez, P.M., Beltran, F.J., Gomez-Serrano, V., Jaramillo, J. and Rodriguez, E.M., 2004. Comparison between thermal and ozone regenerations of spent activated carbon exhausted with phenol. Water Res 38(8), 2155-2165.

Amaral, P., Partlan, E., Li, M., Lapolli, F., Mefford, O.T., Karanfil, T. and Ladner, D.A., 2016. Superfine powdered activated carbon (S-PAC) coatings on microfiltration membranes: Effects of milling time on contaminant removal and flux. Water Research 100, 429-438.

Ando, N., Matsui, Y., Kurotobi, R., Nakano, Y., Matsushita, T. and Ohno, K., 2010. Comparison of natural organic matter adsorption capacities of super-powdered activated carbon and powdered activated Carbon. Water Research 44(14), 4127-4136.

443 Bonvin, F., Jost, L., Randin, L., Bonvin, E. and Kohn, T., 2016. Super-fine powdered
444 activated carbon (SPAC) for efficient removal of micropollutants from wastewater
445 treatment plant effluent. Water Research 90, 90-99.

446 Coimbra, R.N., Calisto, V., Ferreira, C.I.A., Esteves, V.I. and Otero, M., 2015. Removal of
447 pharmaceuticals from municipal wastewater by adsorption onto pyrolyzed pulp mill sludge.
448 Arabian Journal of Chemistry, In Press.

449 Considine, R., Denoyel, R., Pendleton, P., Schumann, R. and Wong, S.-H., 2001. The
450 influence of surface chemistry on activated carbon adsorption of 2-methylisoborneol from
451 aqueous solution. Colloids and Surfaces A: Physicochemical and Engineering Aspects
452 179(2–3), 271-280.

453 Cook, D., Newcombe, G. and Sztajnbok, P., 2001. The application of powdered activated
454 carbon for mib and geosmin removal: predicting pac doses in four raw waters. Water
455 Research 35(5), 1325-1333.

456 Corwin, C.J. and Summers, R.S., 2012. Controlling trace organic contaminants with GAC
457 adsorption. American Water Works Association. Journal 104(1), 43.

458 Croué, J.-P., 2004. Isolation of Humic and Non-Humic NOM Fractions: Structural
459 Characterization. Environmental Monitoring and Assessment 92(1), 193-207.

460 Greenwald, M.J., Redding, A.M. and Cannon, F.S., 2015. A rapid kinetic dye test to predict
461 the adsorption of 2-methylisoborneol onto granular activated carbons and to identify the
462 influence of pore volume distributions. Water Research 68, 784-792.

463 Hu, J., Shang, R., Heijman, B. and Rietveld, L., 2015. Reuse of spent granular activated
464 carbon for organic micro-pollutant removal from treated wastewater. Journal of
465 Environmental Management 160, 98-104.

466 Iwamoto, T., Tasaki, T. and Kanami, T., 2014. Renewal and Selection of Granular
467 Activated Carbon in Advanced Drinking Water Purification in Tokyo, Nagoya, Japan.

468 JWWA, 2005. Powdered activated carbon for water treatment (K 113:2005-2), Japan Water
469 Works Association, Tokyo, Japan.

470 Kameya, T., Hada, T. and Urano, K., 1997. Changes of adsorption capacity and pore
471 distribution of biological activated carbon on advanced water treatment. Water Science and
472 Technology 35(7), 155-162.

473 Kasaoka, S., Sakata, Y., Tanaka, E. and Naitoh, R., 1989. Design of molecular-sieve
474 carbon. Studies on the adsorption of various dyes in the liquid phase. International Journal
475 of Chemical Engineering 29(4), 734-742.

476 Kennedy, A.M., Reinert, A.M., Knappe, D.R.U., Ferrer, I. and Summers, R.S., 2015. Full-
477 and pilot-scale GAC adsorption of organic micropollutants. Water Research 68, 238-248.

478 Kilduff, J.E. and Karanfil, 1998. TCE adsorption by GAC preloaded with humic
479 substances. Journal - American Water Works Association 90(5), 76.

480 Knappe, D.R., Snoeyink, V.L., Roche, P., Prados, M.J. and Bourbigot, M.-M., 1999.
481 Atrazine removal by preloaded GAC. American Water Works Association. Journal 91(10),
482 97.

483 Lambert, S.D., San Miguel, G. and Graham, N.J.D., 2002. Deleterious effects of inorganic
484 compounds DURING THERMAL REGENERATION of GAC: A Review. Journal
485 (American Water Works Association) 94(12), 109-119.

486 Lebeau, T., Lelièvre, C., Wolbert, D., Laplanche, A., Prados, M. and Côté, P., 1999. Effect
487 of natural organic matter loading on the atrazine adsorption capacity of an aging powdered
488 activated carbon slurry. Water Research 33(7), 1695-1705.

489 Li, L., Quinlivan, P.A. and Knappe, D.R.U., 2002a. Effects of activated carbon surface
490 chemistry and pore structure on the adsorption of organic contaminants from aqueous
491 solution. Carbon 40(12), 2085-2100.

492 Li, Q., Snoeyink, V.L., Campos, C. and Mariñas, B.J., 2002b. Displacement Effect of NOM
493 on Atrazine Adsorption by PACs with Different Pore Size Distributions. Environmental
494 Science & Technology 36(7), 1510-1515.

495 Li, Q., Snoeyink, V.L., Mariñas, B.J. and Campos, C., 2003. Pore blockage effect of NOM
496 on atrazine adsorption kinetics of PAC: the roles of PAC pore size distribution and NOM
497 molecular weight. Water Research 37(20), 4863-4872.

498 Lim, J.-L. and Okada, M., 2005. Regeneration of granular activated carbon using
499 ultrasound. Ultrasonics Sonochemistry 12(4), 277-282.

500 Martin, R.J. and Ng, W.J., 1985. Chemical regeneration of exhausted activated carbon—II.
501 Water Research 19(12), 1527-1535.

502 Matsui, Y., Aizawa, T., Kanda, F., Nigorikawa, N., Mima, S. and Kawase, Y., 2007.
503 Adsorptive removal of geosmin by ceramic membrane filtration with super-powdered
504 activated carbon. Journal of Water Supply: Research & Technology-AQUA 56.

505 Matsui, Y., Knappe, D.R.U., Iwaki, K. and Ohira, H., 2002a. Pesticide Adsorption by
506 Granular Activated Carbon Adsorbers. 2. Effects of Pesticide and Natural Organic Matter
507 Characteristics on Pesticide Breakthrough Curves. Environmental Science & Technology
508 36(15), 3432-3438.

Matsui, Y., Knappe, D.R.U. and Takagi, R., 2002b. Pesticide Adsorption by Granular Activated Carbon Adsorbers. 1. Effect of Natural Organic Matter Preloading on Removal Rates and Model Simplification. Environmental Science & Technology 36(15), 3426-3431.

Matsui, Y., Murase, R., Sanogawa, T., Aoki, N., Mima, S., Inoue, T. and Matsushita, T., 2004. Micro-ground powdered activated carbon for effective removal of natural organic matter during water treatment. Water Science & Technology: Water Supply 4(4).

Matsui, Y., Nakano, Y., Hiroshi, H., Ando, N., Matsushita, T. and Ohno, K., 2010. Geosmin and 2-methylisoborneol adsorption on super-powdered activated carbon in the presence of natural organic matter. Water Science & Technology 62(11).

Matsui, Y., Nakao, S., Sakamoto, A., Taniguchi, T., Pan, L., Matsushita, T. and Shirasaki, N., 2015. Adsorption capacities of activated carbons for geosmin and 2-methylisoborneol vary with activated carbon particle size: Effects of adsorbent and adsorbate characteristics. Water Research 85, 95-102.

Matsui, Y., Nakao, S., Taniguchi, T. and Matsushita, T., 2013a. Geosmin and 2-methylisoborneol removal using superfine powdered activated carbon: Shell adsorption and branched-pore kinetic model analysis and optimal particle size. Water research 47(8), 2873-2880.

Matsui, Y., Nakao, S., Yoshida, T., Taniguchi, T. and Matsushita, T., 2013b. Natural organic matter that penetrates or does not penetrate activated carbon and competes or does not compete with geosmin. Separation And Purification Technology 113, 75-82.

Matsui, Y., Sakamoto, A., Nakao, S., Taniguchi, T., Matsushita, T., Shirasaki, N., Sakamoto, N. and Yurimoto, H., 2014. Isotope Microscopy Visualization of the Adsorption Profile of 2-Methylisoborneol and Geosmin in Powdered Activated Carbon. Environmental Science & Technology 48(18), 10897-10903.

Matsui, Y., Yoshida, T., Nakao, S., Knappe, D.R.U. and Matsushita, T., 2012. Characteristics of competitive adsorption between 2-methylisoborneol and natural organic matter on superfine and conventionally sized powdered activated carbons. Water Research 46(15), 4741-4749.

Moreno-Castilla, C., 2004. Adsorption of organic molecules from aqueous solutions on carbon materials. Carbon 42(1), 83-94.

Nakano, Y., Hua, L.Q., Nishijima, W., Shoto, E. and Okada, M., 2000. Biodegradation of trichloroethylene (TCE) adsorbed on granular activated carbon (GAC). Water Research 34(17), 4139-4142.

542 Newcombe, G., Drikas, M. and Hayes, R., 1997. Influence of characterised natural organic
543 material on activated carbon adsorption: II. Effect on pore volume distribution and
544 adsorption of 2-methylisoborneol. Water Research 31(5), 1065-1073.

545 Newcombe, G., Morrison, J. and Hepplewhite, C., 2002a. Simultaneous adsorption of MIB
546 and NOM onto activated carbon. I. Characterisation of the system and NOM adsorption.
547 Carbon 40(12), 2135-2146.

548 Newcombe, G., Morrison, J., Hepplewhite, C. and Knappe, D.R.U., 2002b. Simultaneous
549 adsorption of MIB and NOM onto activated carbon: II. Competitive effects. Carbon 40(12),
550 2147-2156.

551 Owen, D.M., 1998. Removal of DBP precursors by GAC adsorption, American Water
552 Works Association.

553 Pan, L., Matsui, Y., Matsushita, T. and Shirasaki, N., 2016. Superiority of wet-milled over
554 dry-milled superfine powdered activated carbon for adsorptive 2-methylisoborneol
555 removal. Water Research 102, 516-523.

556 Paune, F., Caixach, J., Espadaler, I., Om, J. and Rivera, J., 1998. Assessment on the
557 removal of organic chemicals from raw and drinking water at a Llobregat river water works
558 plant using GAC. Water Research 32(11), 3313-3324.

559 Pelekani, C. and Snoeyink, V.L., 2000. Competitive adsorption between atrazine and
560 methylene blue on activated carbon: the importance of pore size distribution. Carbon
561 38(10), 1423-1436.

562 Quinlivan, P.A., Li, L. and Knappe, D.R.U., 2005. Effects of activated carbon
563 characteristics on the simultaneous adsorption of aqueous organic micropollutants and
564 natural organic matter. Water Research 39(8), 1663-1673.

565 Rey-Mafull, C.A., Tacoronte, J.E., Garcia, R., Tobella, J., Llópiz, J.C., Iglesias, A. and
566 Hotza, D., 2014. Comparative study of the adsorption of acetaminophen on activated
567 carbons in simulated gastric fluid. SpringerPlus 3(1), 1.

568 San Miguel, G., Lambert, S.D. and Graham, N.J.D., 2001. The regeneration of field-spent
569 granular-activated carbons. Water Research 35(11), 2740-2748.

570 Schmit, K.H. and Wells, M.J.M., 2002. Preferential adsorption of fluorescing fulvic and
571 humic acid components on activated carbon using flow field-flow fractionation analysis.
572 Journal of Environmental Monitoring 4(1), 75-84.

573 Scholz, M. and Martin, R.J., 1998. Control of bio-regenerated granular activated carbon by
574 spreadsheet modelling. Journal of Chemical Technology and Biotechnology 71(3), 253-
575 261.

576 Sontheimer, H., Crittenden, J.C., Summers, R.S., Hubele, C., Roberts, C. and Snoeyink,
577 V.L., 1988. Activated carbon for water treatment, Universitaet Karlsruhe, Karlsruhe.

578 Summers, R.S., Kim, S.M., Shimabuku, K., Chae, S.-H. and Corwin, C.J., 2013. Granular
579 activated carbon adsorption of MIB in the presence of dissolved organic matter. Water
580 Research 47(10), 3507-3513.

581 Świetlik, J., Dąbrowska, A., Raczyk-Stanisławiak, U. and Nawrocki, J., 2004. Reactivity of
582 natural organic matter fractions with chlorine dioxide and ozone. Water Research 38(3),
583 547-558.

584 Velten, S., Knappe, D.R.U., Traber, J., Kaiser, H.-P., von Gunten, U., Boller, M. and
585 Meylan, S., 2011. Characterization of natural organic matter adsorption in granular
586 activated carbon adsorbers. Water Research 45(13), 3951-3959.

587 Yu, J., Yang, M., Lin, T.-F., Guo, Z., Zhang, Y., Gu, J. and Zhang, S., 2007. Effects of
588 surface characteristics of activated carbon on the adsorption of 2-methylisobornel (MIB)
589 and geosmin from natural water. Separation and Purification Technology 56(3), 363-370.

590 Zietzschmann, F., Stützer, C. and Jekel, M., 2016. Granular activated carbon adsorption of
591 organic micro-pollutants in drinking water and treated wastewater – Aligning breakthrough
592 curves and capacities. Water Research 92, 180-187.

593

594

Table 1 – Information about the used GACs that were collected.

Designation	Water purification plant	Years used	Raw material	Producer	Production area
KM0-GAC	Kanamachi (Bureau of Waterworks Tokyo Metropolitan Government)	0 (virgin)	Bituminous coal	Norit Japan Co.,Ltd.	USA
KM1-GAC		1 (2012–2013)			
KM2-GAC		2 (2012–2014)			
KM3-GAC		3 (2012–2015)			
KM4-GAC		4 (2007–2011)		Shanxi Xinhua Chemical Co., Ltd	China
KM6-GAC		6 (2006–2012)			
KM9-GAC		9 (2003–2012)	Coal	Calgon Carbon Japan KK.	Japan
AS1-GAC	Asaka (Bureau of Waterworks Tokyo Metropolitan Government)	1 (2014–2015)	Bituminous coal	Unknown	Unknown
AS2-GAC		2 (2013–2015)			
AS7-GAC		7 (2006–2013)	Unknown	Joint venture of Kuraray Chemical Co. ., Ltd and Osaka Gas Chemicals Co., Ltd	Colombia
KS0-GAC	Kasumigaura (Ibaraki Prefectural Government)	0 (regenerated)	Coconut shell	Serachem Co., Ltd	Japan
KS0.1-GAC		0.1 (2016.06–2016.07)			
KS0.3-GAC		0.3 (2016.04–2016.07)			
IS4-GAC	Ishikari (Ishikari-Seibu Water Supply Association)	4 (2012-2016)	Bituminous coal	Dainen Co., Ltd	Japan

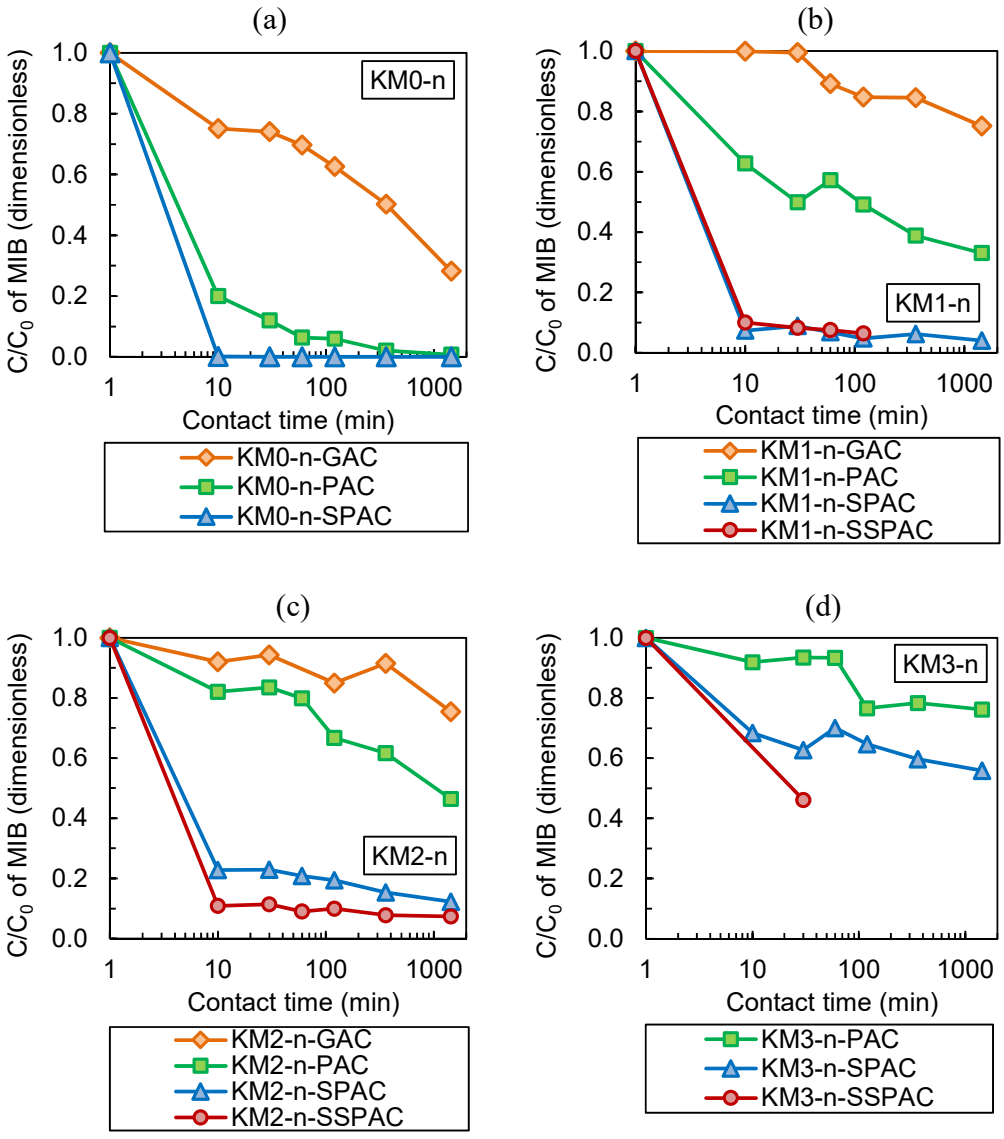

Fig 1 – MIB removal rates against carbon-solution contact time (PAC/SPAC/SSPAC dosage was 40 mg/L in natural water; GAC dosage was 210 ± 10 mg/L in natural water).

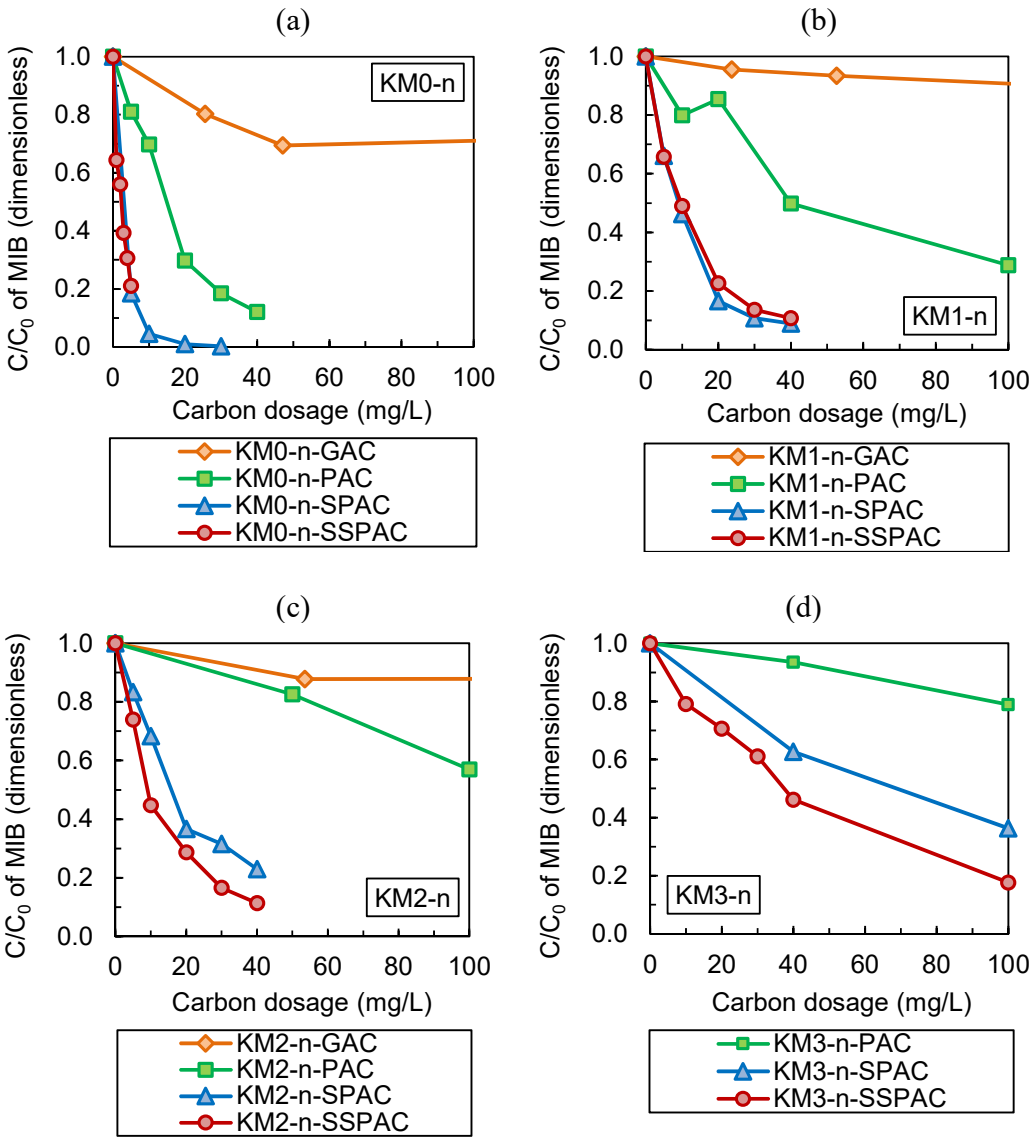

Fig. 2 – MIB removal rates against carbon dosages at a carbon-water contact time of 30 min (natural water).

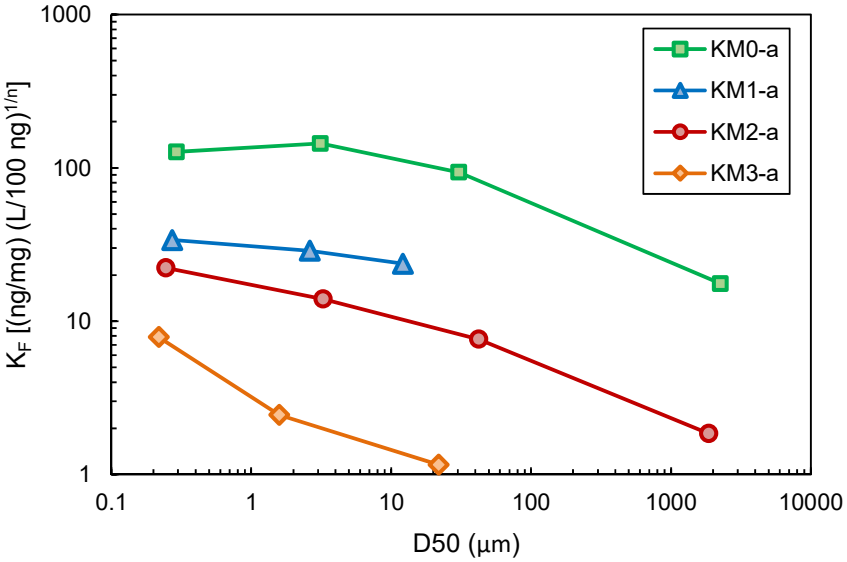

Fig. 3 – MIB adsorption equilibrium capacity versus carbon particle size. The metric of the capacity was the solid-phase concentration in equilibrium with a liquid-phase concentration of 100 ng/L in natural water.

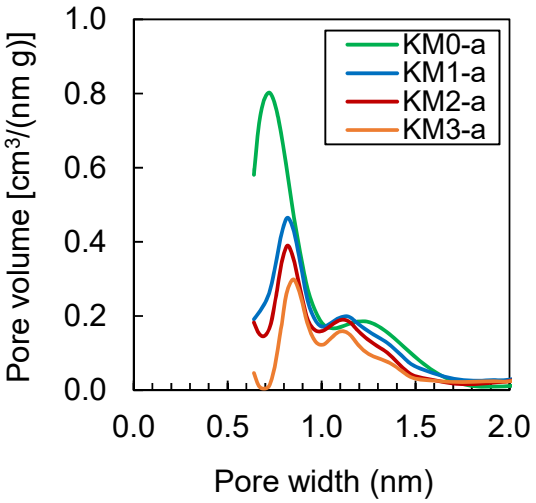

Fig. 4 – Micropore size distributions of KM series carbon.

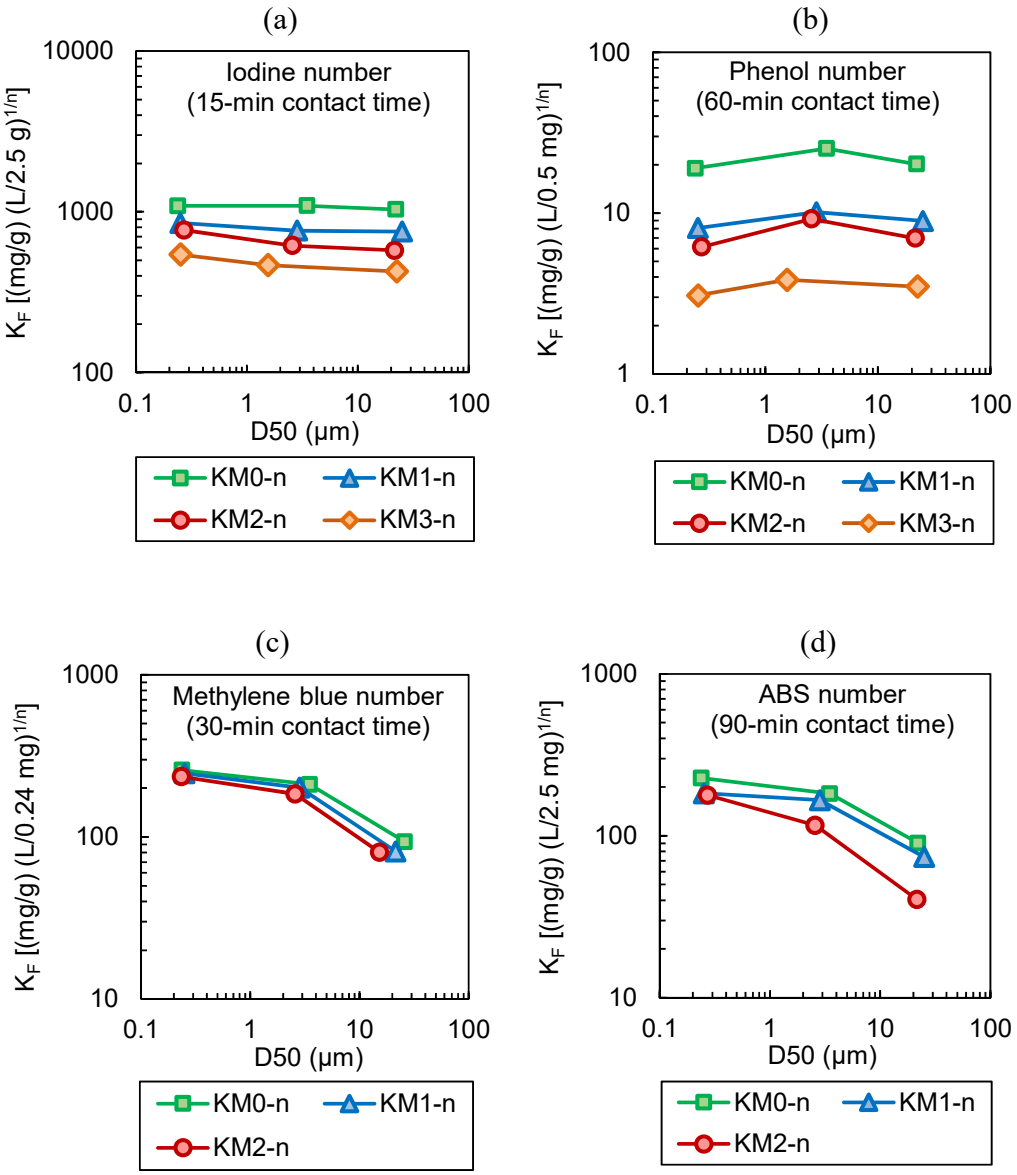

Fig. 5 – Adsorption indices versus carbon particle size.

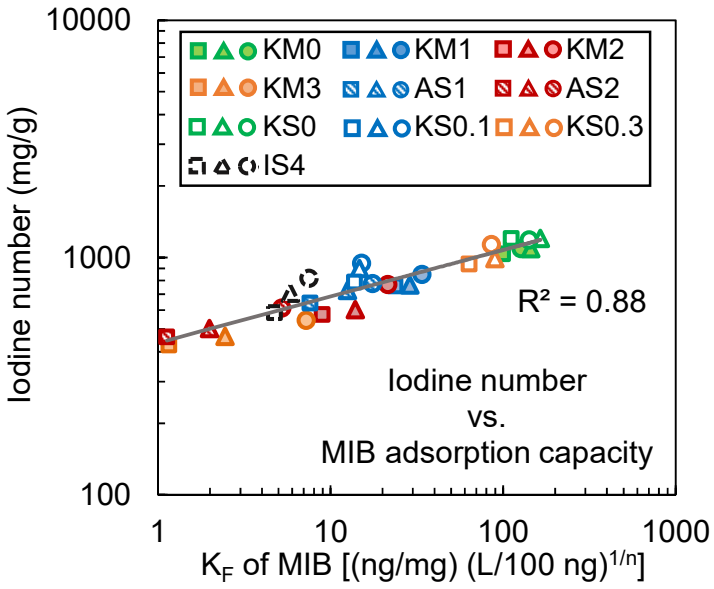

Fig. 6 – Correlation between MIB adsorption capacity and iodine number of carbons. The squares are PACs, the triangles are SPACs, and the circles are SSPACs.

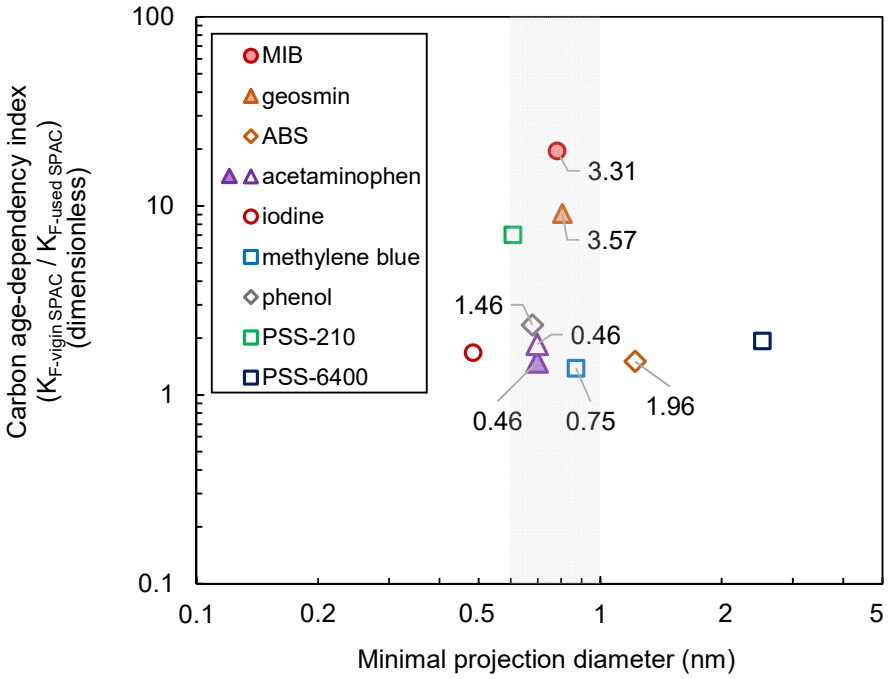

Fig. 7 – Carbon age-dependency index of adsorbates, quantified in terms of the ratio of the adsorption capacity between virgin and used SPAC (D50: 3 µm), against the minimal projection diameter of the adsorbates. Each number in the figure is the log-Kow value of the indicated adsorbate summarized by EPI Suite™ (U.S. Environmental Protection Agency v4.0). The log-Kow of iodine, PSS-210, and PSS-6400 were not obtainable. Closed symbols correspond to data with low initial concentrations (<10 µg/L). Open symbols correspond to data with high initial concentrations (>0.5 mg/L).

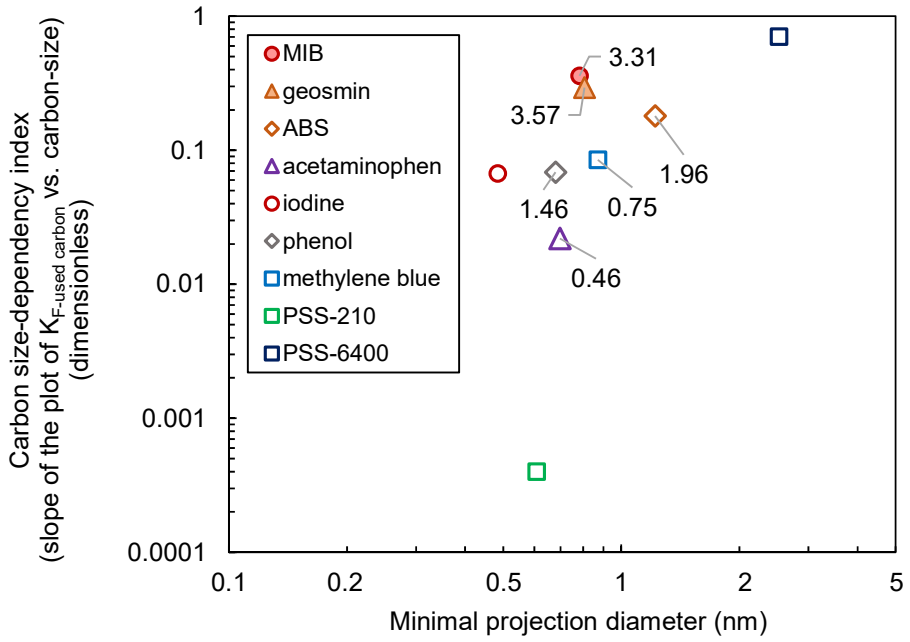

Fig. 8 – Carbon size-dependency index of adsorbates, quantified by the absolute value of the slopes of plots of adsorption capacities of used carbons vs. carbon size, against the minimal projection diameter of the adsorbates. Each number in the figure is the Log-Kow value of each adsorbate summarized by EPI Suite™ (U.S. Environmental Protection Agency v4.0).

Supplementary Information

Micro-milling of Spent Granular Activated Carbon for its Possible Reuse as an Adsorbent: Remaining Capacity and Characteristics

Long Pan [a], Yuichi Takagi [a], Yoshihiko Matsui [b*], Taku Matsushita [b], Nobutaka Shirasaki [b]

a Graduate School of Engineering, Hokkaido University, N13W8, Sapporo 060-8628, Japan
b Faculty of Engineering, Hokkaido University, N13W8, Sapporo 060-8628, Japan

* Corresponding author. Tel./fax: +81-11-706-7280
E-mail address: matsui@eng.hokudai.ac.jp

S1. Preliminary Tests with Used Activated Carbons

S1.1 Samples used in preliminary tests

Preliminary experiments were conducted to briefly observe the removal of MIB by PAC and SPAC produced from GACs that had been used for ≥4 years at water purification plants in Tokyo. The selection of ≥4 years was based on the fact that GACs were replaced every 4–9 years at the water purification plants. SPACs and PACs were produced from GACs by a combination of pulverization with a food processor and a wet-milling bead mill. Table S1 provides relevant information about the carbons.

Table S1 – Carbons used in preliminary tests.

Designation	Parent GAC	Pretreatment of MIB adsorption equilibrium tests	D_{50} (μm)
KM4-n-GAC	KM4-GAC	None	2170
KM4-n-PAC			16.1
KM4-n-SPAC			0.651
KM6-n-GAC	KM6-GAC	None	2100
KM6-n-PAC			22.2
KM6-a-PAC (121 °C)		Autoclave at 121 °C for 15 min	
KM6-a-PAC (63 °C)		Autoclave at 63 °C for 30 min	
KM6-n-SPAC		None	0.725
KM9-n-GAC	KM9-GAC	None	1700
KM9-n-PAC			11.5
KM9-n-SPAC			0.558
AS7-n-GAC	AS7-GAC	None	1290
AS7-n-PAC			10.5
AS7-n-SPAC			0.733
KM2-n-PAC-3	KM2-GAC	None	17.4
KM2-a-PAC		Autoclave at 63 °C for 30 min	42.3
KM2-g-PAC		Gamma ray irradiation under 10.5 ± 0.2 kGy dosage	17.8

S1.2 Effect of biological degradation in isotherm experiments

In the batch adsorption equilibrium tests using the spent GACs and the PAC/SPACs produced from the spent GACs, a two-week contact time was used to allow adsorption to reach equilibrium. This contact time was longer than the time (one week or less) used to obtain MIB adsorption isotherms of PAC/SPAC in previous studies (Graham et al., 2000; Matsui et al., 2015; Newcombe et al., 2002). The reason for choosing a longer contact time was that MIB adsorption by GAC was considered to require a longer contact time to reach adsorption equilibrium than PAC/SPAC due to the larger particle size of GAC and consequently the slow uptake rate. The results were that MIB was not removed by spent GACs and their SPACs, even under the high carbon dosage of 200 mg/L (KM4-n-GAC, KM4-n-SPAC, etc., Fig. S1). However, some of the used carbons with an intermediate size (KM-6-n-PAC, etc.) showed marked MIB removals. These results were obtained for old carbons with ages ≥6 years; more than 90% of the MIB could be removed with a carbon dose of 200 mg/L. Such a high removal was not attained with the 4-year-old carbons.

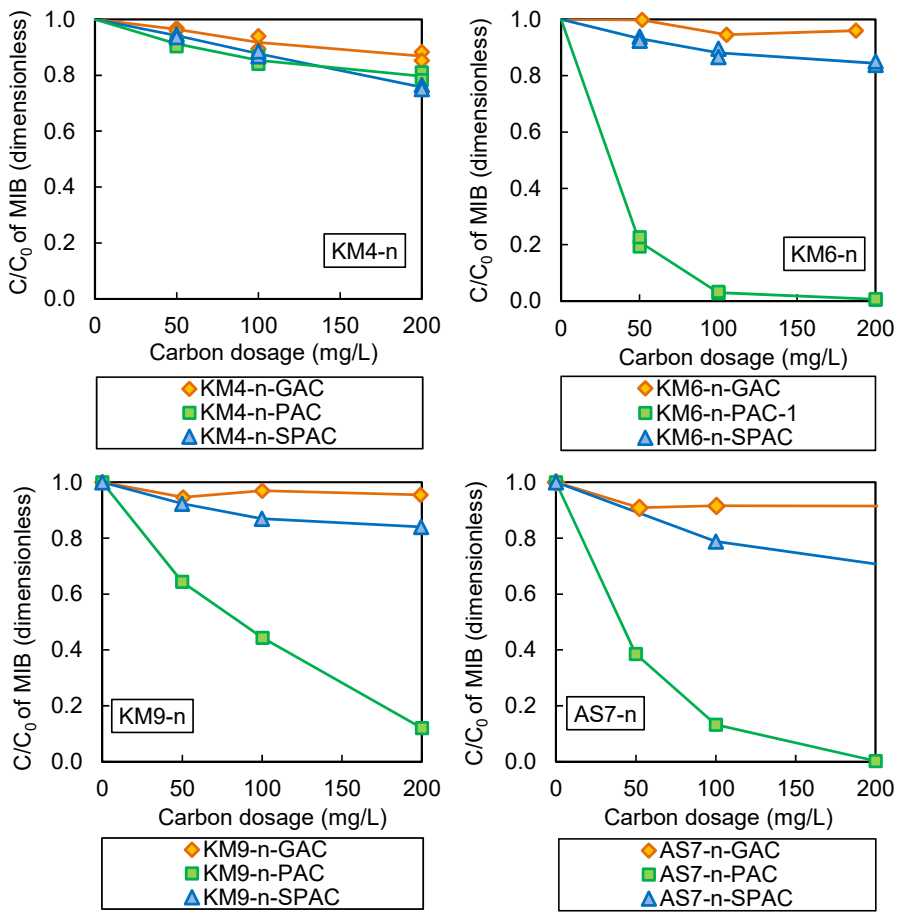

Fig. S1 – MIB removal rates versus carbon dosage at a carbon-water contact time of 2 weeks (natural water).

Among possible reasons why only PAC produced from used carbon ≥ 6 years old achieved high MIB removal, we hypothesized that biological degradation might be the reason, and tested this hypothesis. We observed a change of the liquid-phase MIB concentration with the carbon-solution contact time (Fig. S2). The concentration of MIB did not decline during the initial two days, but it started to decrease after the 3rd day, and for several days the removal rate accelerated. After the MIB concentration reached <5% of the initial concentration on the 14th day, the MIB stock solution was spiked into a carbon-solution system to raise the MIB concentration back to about 1 μg/L, similar to the MIB concentration at the beginning of the experiment. The MIB concentration decreased immediately after the spike. This behavior is typical of biodegradation. We regard the delay of the onset of the decrease of the MIB concentration during the first two days as a reflection of the acclimation period of the bacteria.

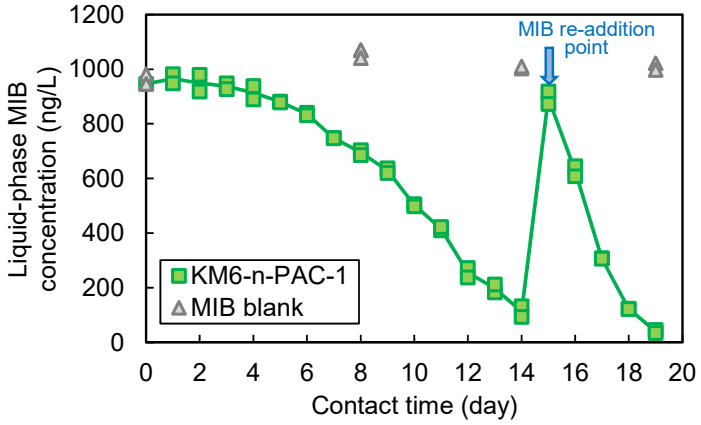

Fig. S2 – Change of MIB concentration after the addition of KM6-n-PAC at a dosage of 100 mg/L in natural water.

S1.3 Sterilization treatment of spent carbons.

To test the biodegradation hypothesis, we sterilized carbons for 30 min and 15 min in an autoclave at 63 °C and 121 °C, respectively. Then we conducted the MIB removal experiments by using the sterilized PACs (KM6-a-PACs), and we carried out a control experiment using un-sterilized PACs (KM6-n-PAC). The MIB concentration did not decrease in the experiment with the sterilized PACs, but it decreased in the experiment with the un-sterilized PACs (Fig. S3). The MIB removals attained with the un-sterilized PACs during very long carbon-solution contact, which is typical of isotherm experiments, were a result of biodegradation. The reason for the lack of MIB removal with spent GACs (Fig. S1) was likely due to the small surface area exposed to the bulk solution. SPACs showed little or no MIB removal as well (Fig. S1), possibly because the bacteria attached to the carbon were physically destroyed in the milling process used to produce the SPAC. SPAC particles are smaller than bacteria. These results also indicated that the MIB adsorption capacity was exhausted after 4 years of service in the water purification plant. We therefore focused on used carbons younger than 4 years in this study.

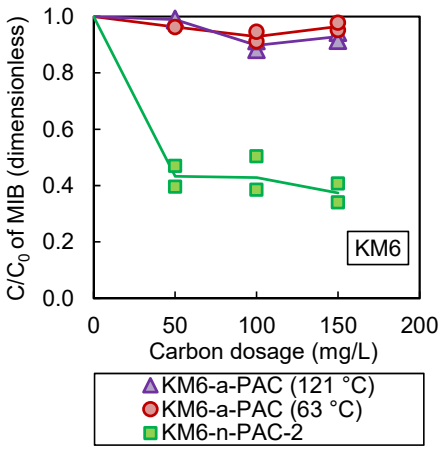

Fig. S3 – Effect of autoclaving on subsequent MIB removal after two-week carbon-water contact time (natural water).

To confirm that there was little effect from autoclaving on the equilibrium MIB adsorption capacity, bottle-point adsorption experiments were conducted with three PACs. KM2-n-PAC was produced by milling two-year-old GAC (KM2-GAC). KM2-a-PAC was produced by autoclaving KM2-n-PAC at 63 °C for 30 min. KM2-g-PAC was produced by sterilizing KM2-n-PAC via gamma ray irradiation at 10.5 ± 0.2 kGy. The MIB removal rates by the three PACs were similar, the indication being that biological degradation of MIB did not occur in the KM2-n-PAC bottles. The lack of biological degradation with the KM2-n-PAC, in contrast to the biological degradation with the KM-6-n-PAC (Fig. S1), could be due to the younger age of the KM2-n-PAC. The similarity of the MIB adsorption isotherms of the three PACs (Fig. S4) suggests that autoclaving and gamma irradiation pretreatment did not modify the carbon characteristics with respect to adsorption capacity. Finally, we used autoclaved carbons in adsorption equilibrium isotherm tests, which require a long carbon-water contact time, in order to avoid any possible biodegradation effect.

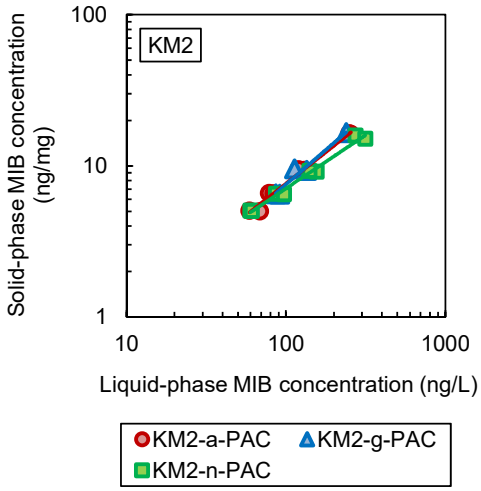

Fig. S4. Effect of autoclaving and gamma irradiation treatments on the adsorption isotherms of MIB in natural water.

S1.4 NOM

The other issue regarding the adsorption experiments with spent carbons was the possibility of NOM desorption from the spent carbons. We monitored the total organic carbon (TOC) and UV absorbance at 260 nm (UV260) of the solution after adding spent carbons (KM9) in natural water supplemented with MIB. In all experiments, the TOC and UV260 did not increase, the indication being that NOM was removed rather than discharged (Fig. S5). Even in the experiment with KM2-n-PAC and organic-free ionic water, the increase of UV260 after a high carbon dosage (200 mg/L) was very small (<0.004 cm^{-1}; no graph attached).

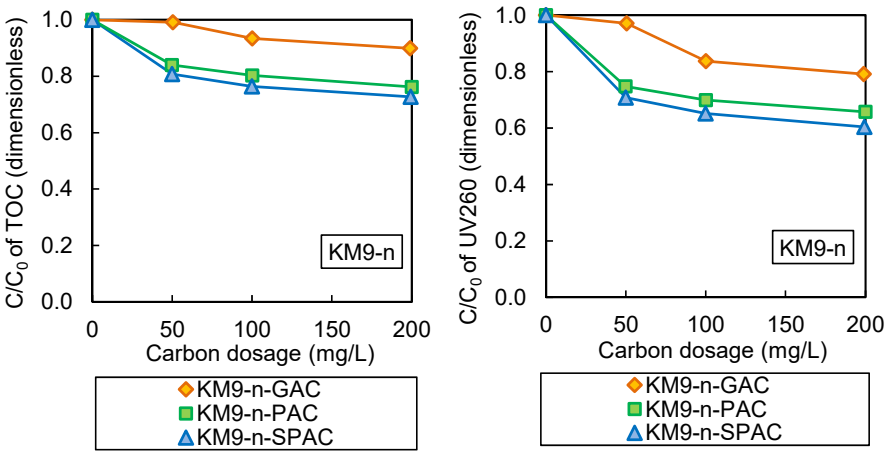

Fig. S5. Change of TOC versus carbon dosage in adsorption equilibrium in natural water. The carbon-water contact time was two weeks. Initial TOC and UV260 were 1.15 ± 0.35 mg/L and 0.045 ± 0.25 cm^{-1}, respectively.

S2. Production of PAC, SPAC, and SSPAC from GAC.

PAC samples were produced from GACs by grinding with a coffee mill under moist conditions followed by grinding with a mortar and pestle under wet conditions after addition of pure water. A 180-μm-sized mesh was used to sieve the ground carbon, and the carbon particles that did not pass the mesh were collected and ground again until they passed the mesh. SPAC with D50 >1.5 μm were produced by milling a PAC slurry in a ball mill (Nikkato Ltd., Osaka, Japan) with a mixture of balls (5-mm and 10-mm balls). To produce SPAC (0.5 μm < D50 <1.5 μm) and SSPAC, the SPAC with D50 >1.5 μm was micro-milled in a bead mill (LMZ015, Ashizawa Finetech Ltd., Chiba, Japan; bead diameter, 0.1 mm).

The particle size (as projected-area diameter) distribution of the GAC was determined by image analysis of pictures taken through a microscope (Viewtrac, MicrotracBEL Corp., Osaka, Japan). Particle size distributions of the SPACs and PACs were determined by using a laser-light-scattering instrument (Microtrac MT3300EXII, Nikkiso Co., Tokyo, Japan) after addition of a dispersant (Triton X-100, Kanto Chemical Co., Tokyo, Japan; final concentration, 0.8 g/L) and subsequent ultrasonic dispersion. Fig. S6 shows the size distributions of the carbons used in the main experiments.

(a)

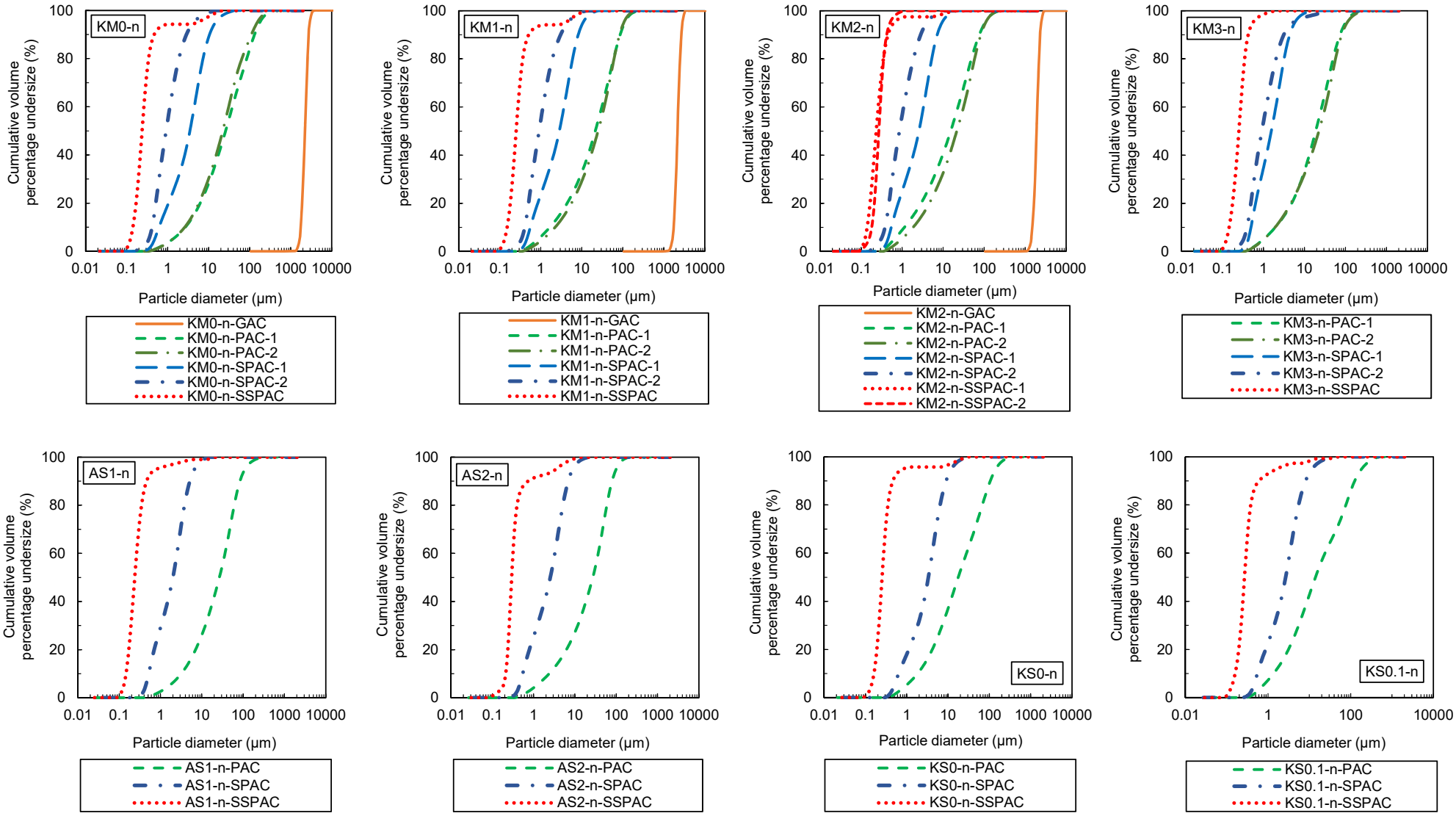
KM0-n
Cumulative volume percentage undersize (%)
Particle diameter (μm)
KM0-n-GAC
KM0-n-PAC-1
KM0-n-PAC-2
KM0-n-SPAC-1
KM0-n-SPAC-2
KM0-n-SSPAC
KM1-n
KM1-n-GAC
KM1-n-PAC-1
KM1-n-PAC-2
KM1-n-SPAC-1
KM1-n-SPAC-2
KM1-n-SSPAC
KM2-n
KM2-n-GAC
KM2-n-PAC-1
KM2-n-PAC-2
KM2-n-SPAC-1
KM2-n-SPAC-2
KM2-n-SSPAC-1
KM2-n-SSPAC-2
KM3-n
KM3-n-PAC-1
KM3-n-PAC-2
KM3-n-SPAC-1
KM3-n-SPAC-2
KM3-n-SSPAC
AS1-n
AS1-n-PAC
AS1-n-SPAC
AS1-n-SSPAC
AS2-n
AS2-n-PAC
AS2-n-SPAC
AS2-n-SSPAC
KS0-n
KS0-n-PAC
KS0-n-SPAC
KS0-n-SSPAC
KS0.1-n
KS0.1-n-PAC
KS0.1-n-SPAC
KS0.1-n-SSPAC

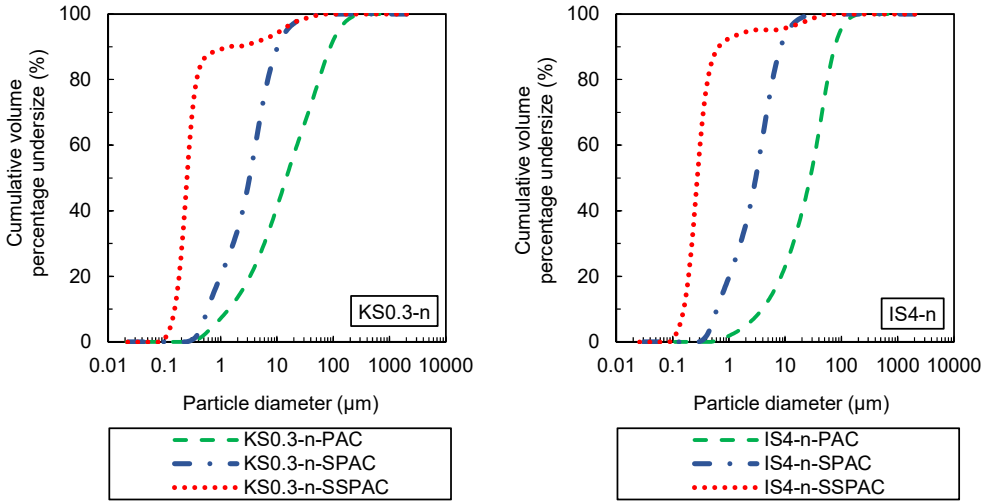
Cumulative volume percentage undersize (%)
Particle diameter (μm)
KS0.3-n
KS0.3-n-PAC
KS0.3-n-SPAC
KS0.3-n-SSPAC
IS4-n
IS4-n-PAC
IS4-n-SPAC
IS4-n-SSPAC

(b)

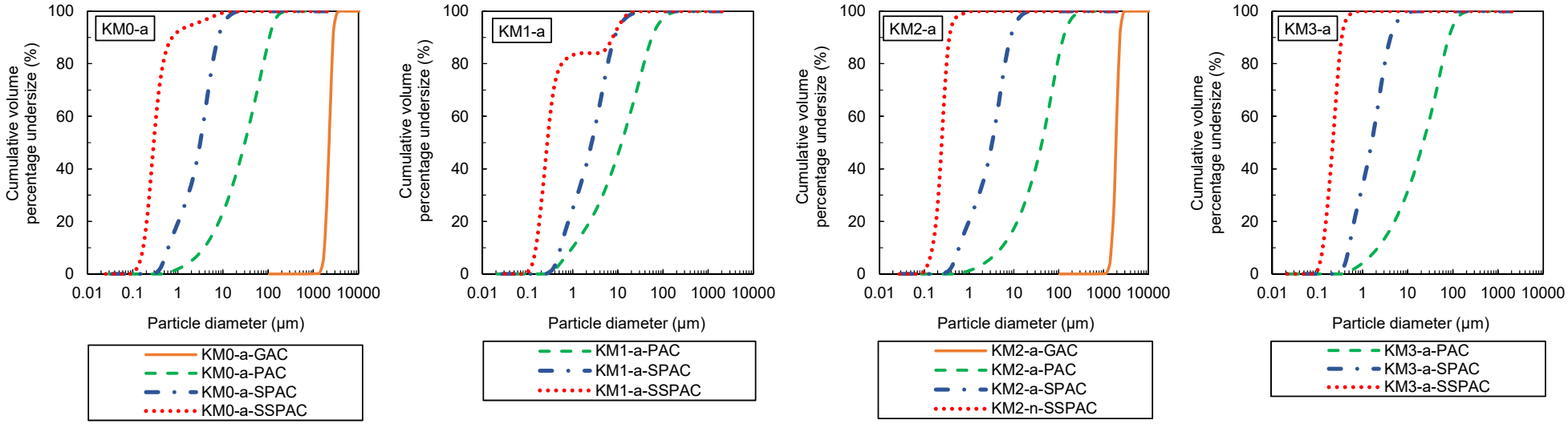
KM0-a
KM0-a-GAC
KM0-a-PAC
KM0-a-SPAC
KM0-a-SSPAC
KM1-a
KM1-a-PAC
KM1-a-SPAC
KM1-a-SSPAC
KM2-a
KM2-a-GAC
KM2-a-PAC
KM2-a-SPAC
KM2-n-SSPAC
KM3-a
KM3-a-PAC
KM3-a-SPAC
KM3-a-SSPAC

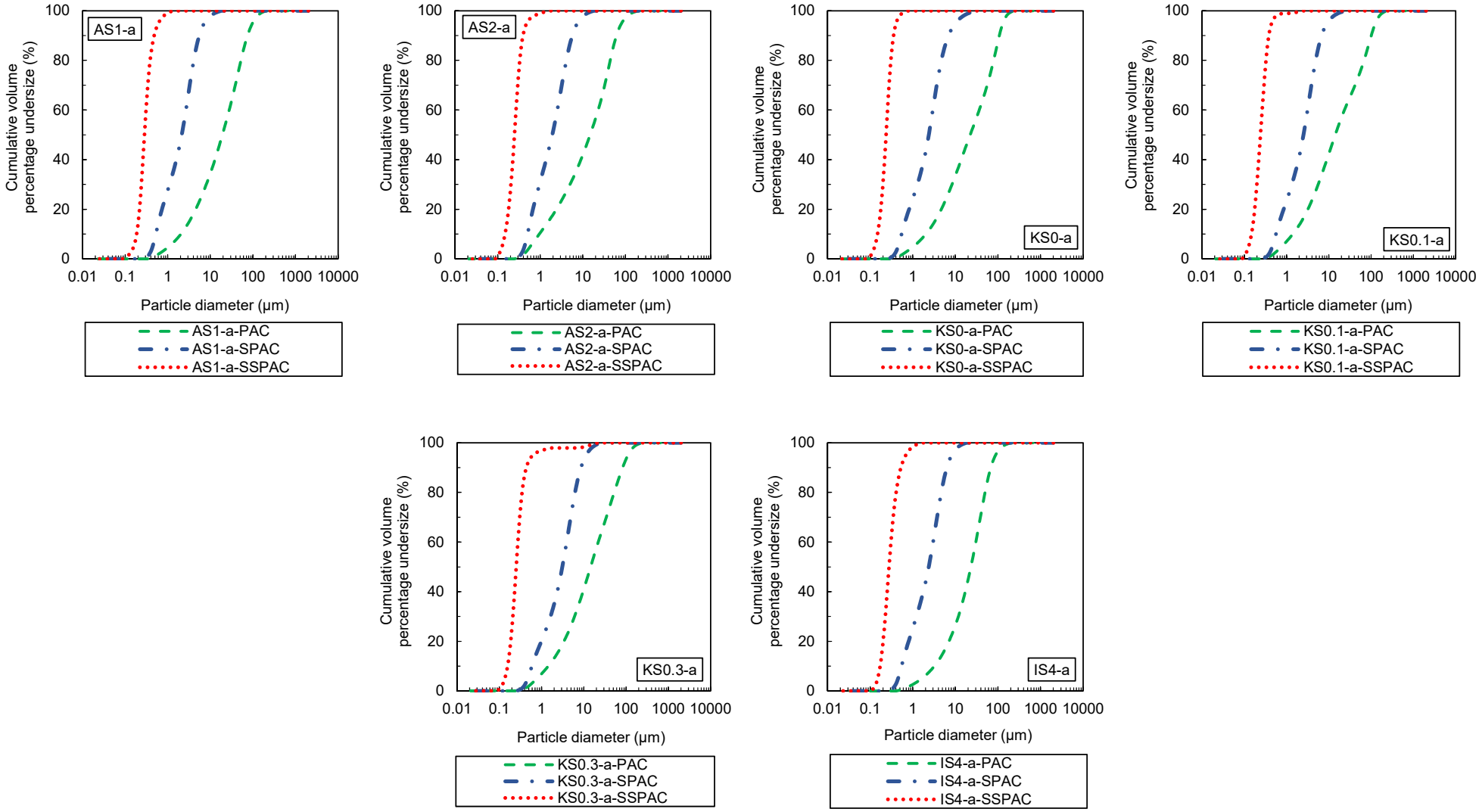

Fig. S6 – Particle size distributions of GAC/PAC/SPAC/SSPAC used in main experiments.

Table S2 – No-autoclave pretreated carbons used for MIB kinetics and adsorption index experiments.

Designation	Parent GAC	Applied experiments	D_{50} (μm)
KM0-n-GAC	KM0-n-GAC	MIB adsorption kinetics	2240
KM0-n-PAC-1		MIB adsorption kinetics; Methylene blue (MB) number	25.9
KM0-n-PAC-2		Iodine number; Phenol number; sodium liner-dodecylbenzene sulfonate (ABS) number	22.1
KM0-n-SPAC-2		MIB adsorption kinetics	0.917
KM0-n-SPAC-1		Iodine number; Phenol number; MB number; ABS number	3.49
KM0-n-SSPAC		MIB adsorption kinetics; Iodine number; Phenol number; MB number; ABS number	0.238
KM1-n-GAC	KM1-n-GAC	MIB adsorption kinetics	2170
KM1-n-PAC-1		MIB adsorption kinetics; MB number	21.5
KM1-n-PAC-2		Iodine number; Phenol number; ABS number	25.1
KM1-n-SPAC-2		MIB adsorption kinetics	0.911
KM1-n-SPAC-1		Iodine number; Phenol number; MB number; ABS number	2.84
KM1-n-SSPAC		MIB adsorption kinetics; Iodine number; Phenol number; MB number; ABS number	0.251
KM2-n-GAC	KM2-n-GAC	MIB adsorption kinetics	1910
KM2-n-PAC-1			15.3
KM2-n-PAC-2		Iodine number; Phenol number; MB number; ABS number	21.5
KM2-n-SPAC-2		MIB adsorption kinetics	0.860
KM2-n-SPAC-1		Iodine number; Phenol number; MB number; ABS number	2.57
KM2-n-SSPAC-1		MIB adsorption kinetics; MB number	0.234
KM2-n-SSPAC-2		Iodine number; Phenol number, ABS number	0.271
KM3-n-PAC-1	KM3-n-GAC	MIB adsorption kinetics	18.8
KM3-n-PAC-2		Iodine number; Phenol number	22.5
KM3-n-SPAC-2		MIB adsorption kinetics;	0.912
KM3-n-SPAC-1		Iodine number; Phenol number	1.56
KM3-n-SSPAC		MIB adsorption kinetics; Iodine number; Phenol number	0.252
AS1-n-PAC	AS1-n-GAC	Iodine number	26.6
AS1-n-SPAC			1.99
AS1-n-SSPAC			0.237
AS2-n-PAC	AS2-n-GAC		27.1
AS2-n-SPAC			2.53
AS2-n-SSPAC			0.294
KS0-n-PAC	KS0-n-GAC		17.6
KS0-n-SPAC			3.34
KS0-n-SSPAC			0.253
KS0.1-n-PAC	KS0.1-n-GAC		14.0
KS0.1-n-SPAC			2.65
KS0.1-n-SSPAC			0.268
KS0.3-n-PAC	KS0.3-n-GAC		14.6
KS0.3-n-SPAC			3.24
KS0.3-n-SSPAC			0.251
IS4-n-PAC	IS4-n-GAC		27.8
IS4-n-SPAC			2.99
IS4-n-SSPAC			0.274

Table S3 – Autoclave-pretreated carbons used for adsorption equilibrium experiments.

Designation	Parent GAC	Applied experiments	D_{50} (μm)
KM0-a-GAC	KM0-a-GAC	Adsorption equilibrium of MIB in natural water	2240
KM0-a-PAC		Adsorption equilibrium of MIB in natural water; Adsorption equilibrium of MIB, geosmin, acetaminophen, phenol, poly(styrenesulfonic acid) sodium salt MW210 (PSS-210), PSS-6400, MB, ABS in organic-free ionic water; N_2 adsorption (Pore size distribution)	31.1
KM0-a-SPAC			3.13
KM0-a-SSPAC			0.293
KM1-a-PAC	KM1-a-GAC	Adsorption equilibrium of MIB in natural water; N_2 adsorption (Pore size distribution)	12.1
KM1-a-SPAC			2.63
KM1-a-SSPAC			0.273
KM2-a-GAC	KM2-a-GAC	Adsorption equilibrium of MIB in natural water	1910
KM2-a-PAC		Adsorption equilibrium of MIB in natural water; Adsorption equilibrium of MIB, geosmin, acetaminophen, phenol, PSS-210, PSS-6400, MB, ABS in organic-free ionic water; N_2 adsorption (Pore size distribution)	42.3
KM2-a-SPAC			3.28
KM2-a-SSPAC			0.246
KM3-a-PAC	KM3-a-GAC	Adsorption equilibrium of MIB in natural water; N_2 adsorption (Pore size distribution)	21.9
KM3-a-SPAC			1.59
KM3-a-SSPAC			0.218
AS1-a-PAC	AS1-a-GAC	Adsorption equilibrium of MIB in natural water	19.2
AS1-a-SPAC			2.13
AS1-a-SSPAC			0.284
AS2-a-PAC	AS2-a-GAC		14.8
AS2-a-SPAC			1.91
AS2-a-SSPAC			0.248
KS0-a-PAC	KS0-a-GAC		22.3
KS0-a-SPAC			2.38
KS0-a-SSPAC			0.236
KS0.1-a-PAC	KS0.1-a-GAC		14.2
KS0.1-a-SPAC			2.51
KS0.1-a-SSPAC			0.241
KS0.3-a-PAC	KS0.3-a-GAC		14.5
KS0.3-a-SPAC			3.10
KS0.3-a-SSPAC			0.252
IS4-a-PAC	IS4-a-GAC		23.1
IS4-a-SPAC			2.37
IS4-a-SSPAC			0.277

S3. Absorbability indices

The amounts of iodine, phenol, MB, and ABS adsorbed onto the carbons at specified liquid-phase concentrations after specified adsorbate-adsorbent contact times were termed the iodine number, phenol number, MB number, and ABS number, respectively. The iodine number was equated to the solid-phase concentration at equilibrium with a liquid-phase concentration of 2.5 g/L after a 15-min contact time in working solution A (see section S5); the phenol number was equated to the solid-phase concentration measured after a 60-min contact time in working solution C with a liquid-phase concentration of 0.5 mg/L; the MB number was equated to the solid-phase concentration after a 30-min contact time in working solution D at a liquid-phase concentration of 0.24 mg/L; the ABS number was equated to the solid-phase concentration after a 90-min contact time in working solution A at a liquid-phase concentration of 2.5 mg/L. These values were measured according to the standard methods of the Japan Water Works Association (K 113:2005-2) (JWWA, 2005).

Measurement methods for the iodine number and MB number:
A carbon slurry was added to an Erlenmeyer flask that contained 25-mL of 6.35-g/L iodine in an iodine/KI solution or 24 mg/L of MB in a phosphate-buffer solution. After shaking for 15 min for iodine adsorption or 30 min for MB adsorption at 100 rpm at 20 °C, the mixed carbon-solution suspensions were each filtered through a 0.2-μm pore size membrane filter (DISMIC-25HP; Toyo Roshi Kaisha, Ltd., Tokyo, Japan, SSPAC-solution suspension was filtered twice). The concentrations of iodine or MB in the aqueous phase were then measured by titration or spectrophotometry, respectively. The solid-phase concentrations of iodine adsorbed onto the carbon samples at a liquid-phase concentration of 2.5 g/L were calculated based on the obtained adsorption isotherms and defined as iodine numbers. Similarly, the MB number was the carbon solid-phase concentration of MB at a liquid-phase concentration 0.24 mg/L.

Measurement methods for phenol number and ABS number:
Carbon slurries were added to 110-mL vials that contained 1-mg/L phenol in an organic-free ionic solution or 5 mg/L of ABS in pure water. After shaking for 90 min (ABS) or 60 min (phenol) at 100 rpm at 20 °C, the carbon-solution suspensions were each filtered through a 0.2-μm pore size membrane filter (the SSPAC-solution suspension was filtered twice), and then the concentrations of phenol or ABS in the aqueous phase were measured by spectrophotometry. The phenol number and ABS number were equated to the carbon solid-phase concentration of phenol and ABS at liquid-phase concentrations of 0.5 mg/L and 2.5 mg/L, respectively.

S4. Working Solutions and Batch Adsorption Tests

Four working solutions were prepared and used in this research. Solution A was ultrapure water obtained from a Milli-Q Advantage (Millipore Co., Bedford, MA, USA). Solution B (natural water) was the raw water of the Kanamachi Water Purification Plant, the same plant where we collected the virgin and used carbons that were the main targets of this study. Table S4 provides information about the ion concentrations, dissolved organic carbon (DOC), and other related information about this water. Solution C (organic-free ionic water) was made from ultrapure water by adding ions at the same concentrations found in the natural water (working solution B). Working solutions B and C were each filtered through a 0.2-μm pore size membrane filter (Advantec H020A; Toyo Roshi Kaisha, Ltd., Tokyo, Japan), and the pH was adjusted to 7.0 ± 0.1 before the solutions were used in the adsorption experiments. Solution D (phosphate buffer water) was a mixture of potassium dihydrogen phosphate (KH_2PO_4) and potassium monohydrogen phosphate (K_2HPO_4) dissolved in ultrapure water; the pH was maintained at 7.0 ± 0.1.

Working solutions B and C were used for the MIB adsorption experiments after adjusting the concentrations of MIB to about 1 μg/L, because MIB usually occurs naturally at concentrations lower than 1 μg/L. The concentration of geosmin in working solution C was also set to about 1 μg/L for the adsorption experiments. In the adsorption tests with iodine, iodine was dissolved in working solution A together with potassium iodide at 6.35 g-I/L. Starch was used as an indicator. The adsorption experiments with MB were conducted in working solution D because of the pH-dependent characteristics of MB; the MB concentrations were 24 and 0.48 mg/L. Working solutions A and C were used for ABS experiments; the concentration of ABS was 5 mg/L. The other compounds were dissolved in working solution C at appropriate concentrations based on the range of concentrations within which individual compounds could be measured with a UV-VIS spectrophotometer: phenol: 1 mg/L; acetaminophen: 2 mg/L; PSS-210 and PSS-6400: 4 mg/L. An adsorption experiment with acetaminophen at 10 μg/L (low concentration) was also conducted.

In all adsorption kinetics and equilibrium tests, aliquots (100 or 110 mL) of the working solutions containing the target compounds were transferred to 110-mL vials. Specified amounts of carbon were immediately added, and the vials were manually shaken and then agitated on a mechanical shaker to keep shaking for a pre-determined period of time at a constant temperature of 20 °C in the dark. After the pre-determined carbon-solution contact time, the carbon-solution mixtures were each filtered through a 0.2-μm pore size membrane filter (SSPAC-solution mixture was filtered twice), and the concentrations of the adsorbate in the aqueous phase were measured. The carbon-solution contact time ranged from 10 minutes to 24 hours for MIB adsorption kinetics experiments, but it was set to two weeks for the MIB adsorption equilibrium

experiments with natural water (working solution B) because of the slow rate of adsorption onto GAC and used carbons in natural water. Adsorption experiments in organic-free ionic water (working solution C) were conducted with PAC, SPAC, and SSPAC to check the adsorption capacity of single target compounds when there was no adsorption competition. The carbon-solution contact time for adsorption equilibrium in organic-free ionic water was shortened to 7 days for all compounds except phenol (0.5 days), acetaminophen of low concentration (0.5 days), and iodine (15 min) while adsorption equilibria were confirmed.

Table S4 – Information about the natural water (working solution B)

pH	Turbidity	Ammonia nitrogen	Conductivity	$KMnO_4$ consumption
7.8	14 NTU	0.04 mg/L	27 μS/m	8.8 mg/L
Alkalinity	DOC	UV260	MIB	Geosmin
48 mg/L	1.2 mg/L	0.04 cm^{-1}	5 ng/L	Undetectable

Ion	Na^+	K^+	Mg^{2+}	Ca^{2+}	Cl^-	NO_3^-	SO_4^{2-}
Concentration (mg/L)	20	3.8	4.9	24	8.0	4.1	31

S5. Analytical Methods for the Supplementary Compounds

Geosmin was detected with a method similar to the method used to detect MIB: the *m/z* 112 peak was assumed to correspond to geosmin. Iodine concentrations were measured by titration with sodium thiosulfate ($Na_2S_2O_3$). The concentrations of other adsorbates were measured by spectrophotometry (UV-1800, Shimadzu Co., Kyoto, Japan): phenol at 269.5 nm; high concentrations of acetaminophen (~2 mg/L) at 244 nm; PSS-210 and PSS-6400 at 261 nm; and MB at 665 nm. Concentrations of ABS were measured by spectrophotometry at 223.5 nm or by TOC analyzer (Sievers 900, Ionics Instrument Business Grp., Boulder Co.). The choice of method was based on the working solutions in the experiments because of the effect of ions on spectrophotometry at wavelengths less than 240 nm. Low concentrations of acetaminophen (~10 µg/L) were quantified by using a hybrid quadrupole-orbitrap mass spectrometer (Q Exactive, Thermo Fisher Scientific Inc., Waltham, MA, USA) coupled with liquid chromatography (UltiMate3000 LC systems, Thermo Fischer Scientific Inc.).

S6. Other Supplementary Data

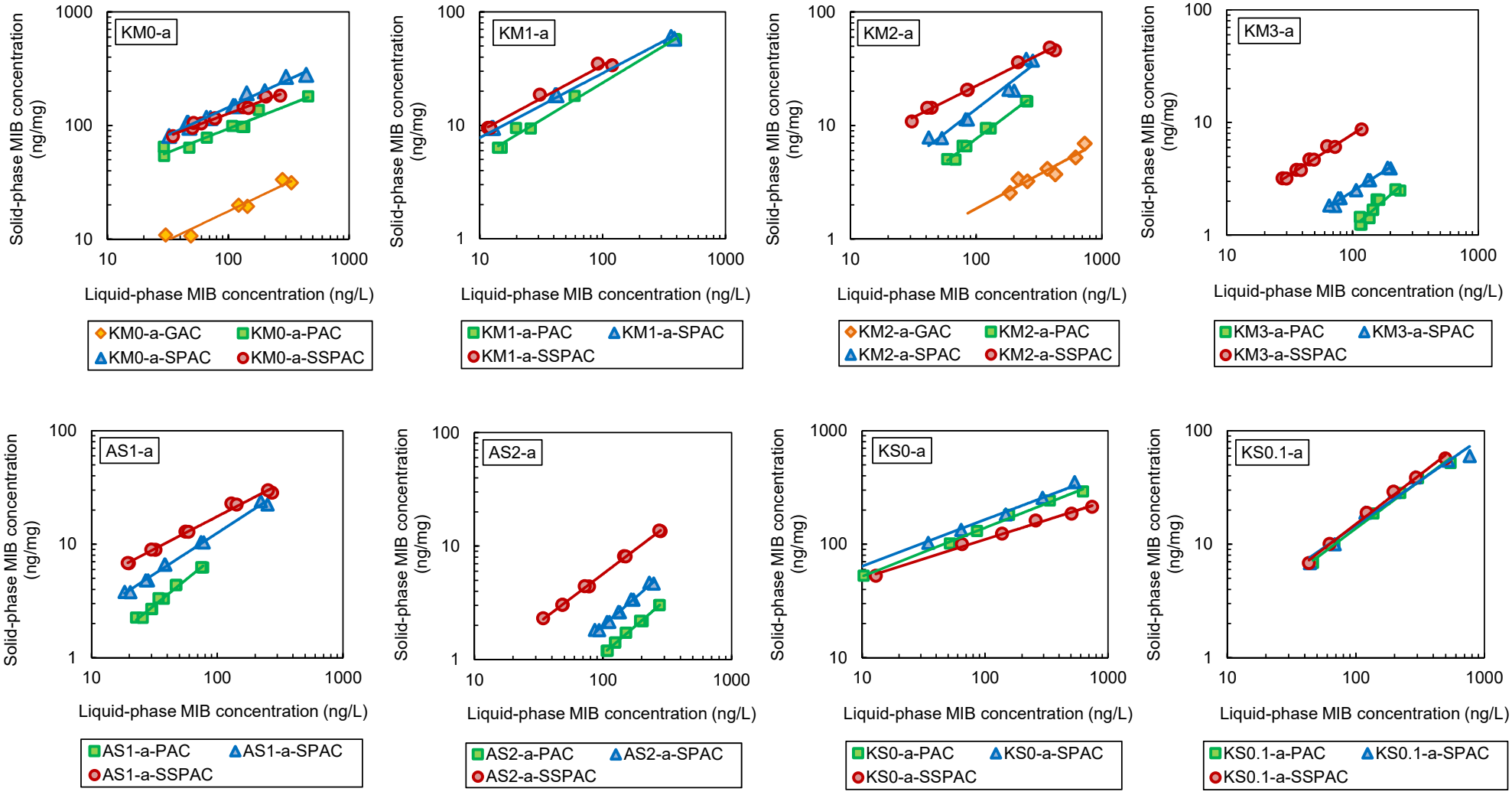

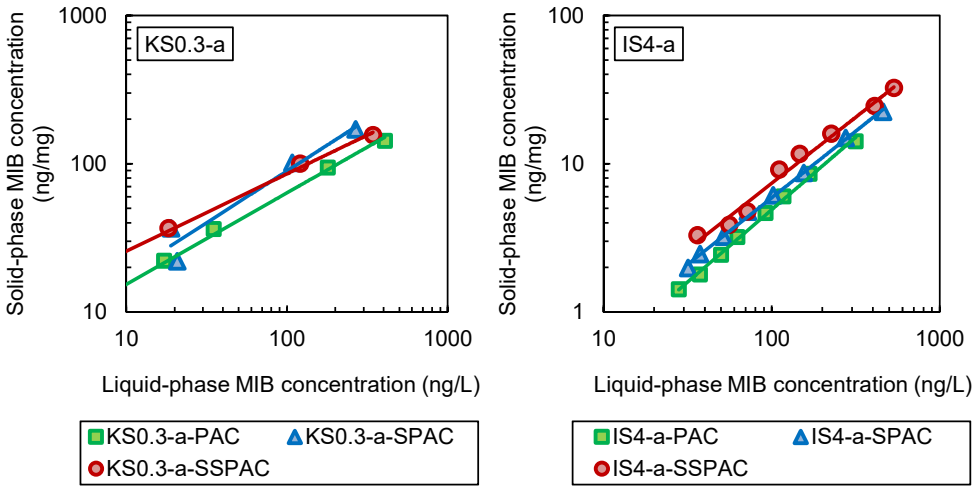

Fig. S7 – MIB adsorption isotherms in natural water. (The parameter values of Freudlich model equations fitted by experimental data are list in Table S5)

Table S5 –The parameter values of Freundlich model equation

$q = K_F\, c^{1/n}$, where q is solid-phase concentrations (ng/mg), c is liquid-phase concentration (ng/L), K_F is the Freundlich capacity parameter [(ng/mg)/(L/ng)$^{1/n}$], and n is Freundlich exponent (dimensionless).

			K_F [(ng/mg)/(L/ng)$^{1/n}$]	K_F [(ng/mg)/(L/100 ng)$^{1/n}$]	$1/n$ (dimensionless)
KM	KM0	KM0-a-GAC	1.69	17.6	0.508
		KM0-a-PAC	13.7	93.6	0.418
		KM0-a-SPAC	15.2	144	0.489
		KM0-a-SSPAC	20.3	127	0.398
	KM1	KM1-a-PAC	1.17	23.7	0.654
		KM1-a-SPAC	2.10	28.8	0.569
		KM1-a-SSPAC	2.30	33.8	0.583
	KM2	KM2-a-GAC	0.117	1.85	0.600
		KM2-a-PAC	0.164	7.62	0.833
		KM2-a-SPAC	0.269	13.9	0.857
		KM2-a-SSPAC	1.74	22.3	0.553
	KM3	KM3-a-PAC	0.013	1.16	0.978
		KM3-a-SPAC	0.091	2.44	0.714
		KM3-a-SSPAC	0.285	7.88	0.721
AS	AS1	AS1-a-PAC	0.130	8.13	0.898
		AS1-a-SPAC	0.453	12.5	0.721
		AS1-a-SSPAC	1.25	17.5	0.574
	AS2	AS2-a-PAC	0.013	1.12	0.974
		AS2-a-SPAC	0.022	1.98	0.981
		AS2-a-SSPAC	0.110	5.68	0.857
KS	KS0	KS0-a-PAC	19.3	139	0.429
		KS0-a-SPAC	24.8	165	0.411
		KS0-a-SSPAC	22.8	110	0.342
	KS0.1	KS0.1-a-PAC	0.282	13.7	0.844
		KS0.1-a-SPAC	0.389	14.6	0.788
		KS0.1-a-SSPAC	0.273	15.0	0.871
	KS0.3	KS0.3-a-PAC	3.71	63.6	0.617
		KS0.3-a-SPAC	3.60	89.2	0.697
		KS0.3-a-SSPAC	7.72	85.5	0.522
IS	IS4	IS4-a-PAC	0.055	4.90	0.977
		IS4-a-SPAC	0.094	5.89	0.899
		IS4-a-SSPAC	0.122	7.38	0.892

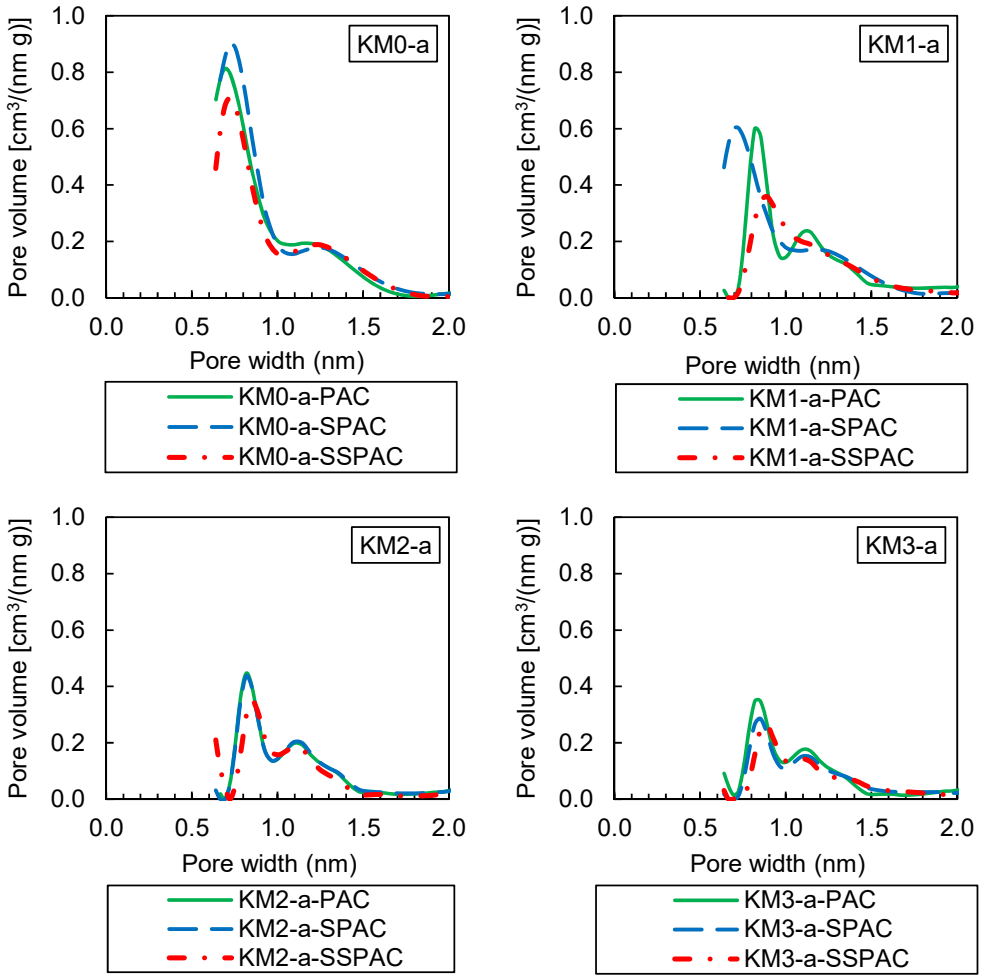

Fig. S8 – Micropore size distributions of PAC, SPAC, and SSPAC.

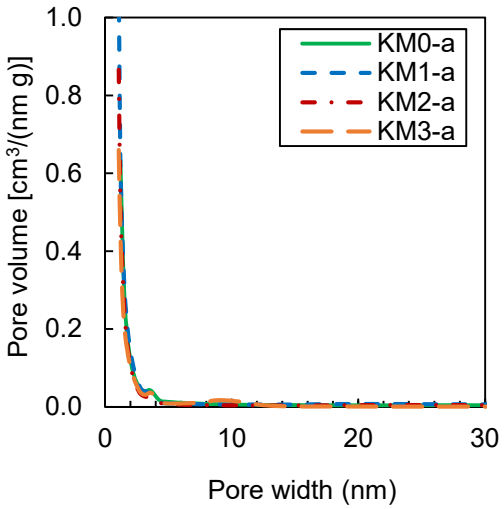

Fig. S9 – Mesopore size distributions of KM-series carbon.

Table S6 –The BET surface areas of KM-series carbon

	BET surface area (m^2/g)
KM0-a	1082 ± 23.3
KM1-a	969 ± 35.6
KM2-a	828 ± 26.9
KM3-a	672 ± 53.1

The BET (Brunauer-Emmett-Teller) surface areas were the average values of PAC, SPAC, and SSPAC of the same age. The value of each carbon was obtained by using the nitrogen gas adsorption-desorption method (Autosorb-iQ, Quantachrome Instruments, Kanagawa, Japan). The isotherm data for nitrogen gas desorption at 77.4 K were analyzed with the BET equation (ASiQwin, ver.3.01, Quantachrome Instruments).

(a) (Iodine)

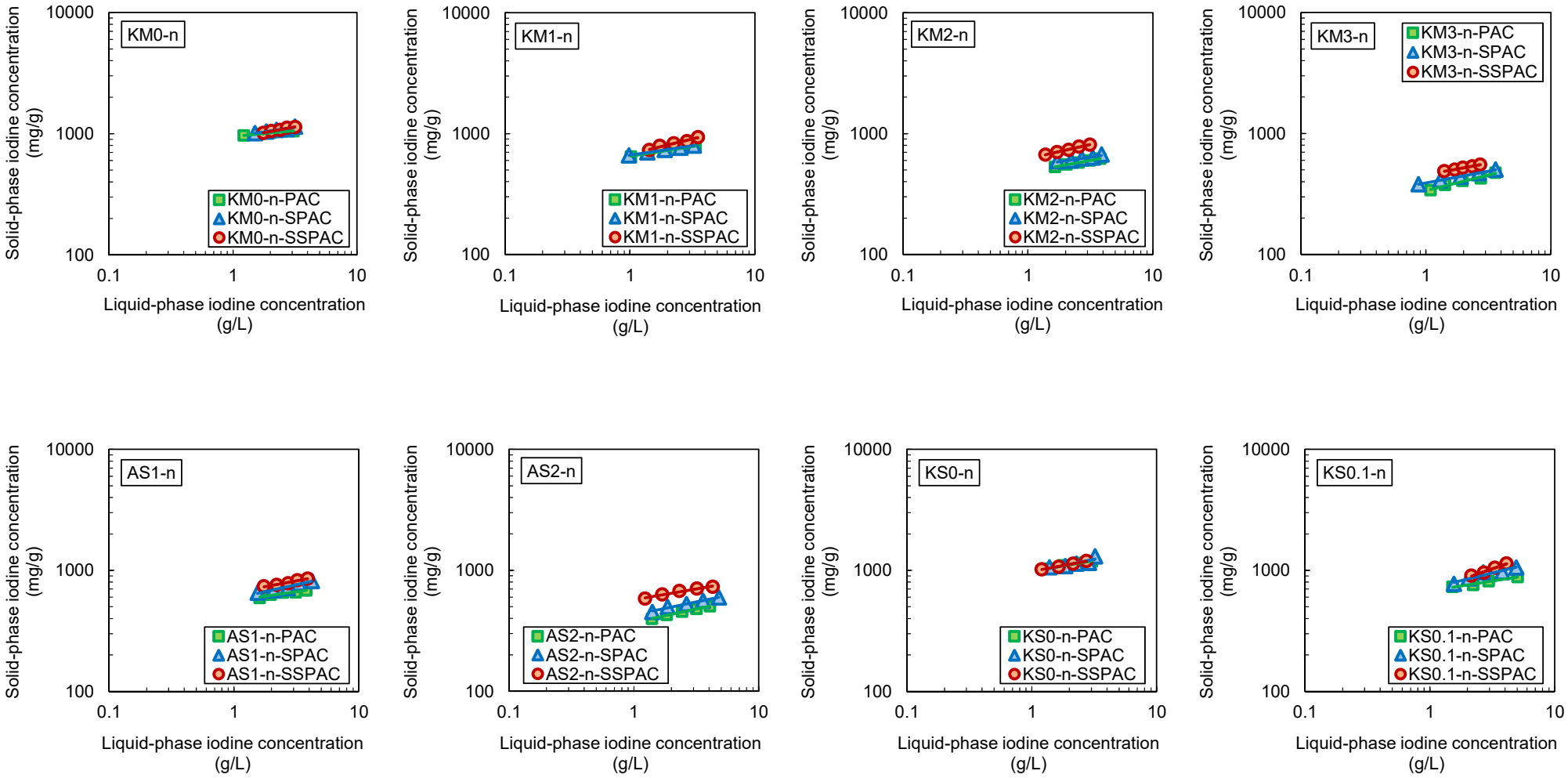
KM0-n
KM0-n-PAC
KM0-n-SPAC
KM0-n-SSPAC
KM1-n
KM1-n-PAC
KM1-n-SPAC
KM1-n-SSPAC
KM2-n
KM2-n-PAC
KM2-n-SPAC
KM2-n-SSPAC
KM3-n
KM3-n-PAC
KM3-n-SPAC
KM3-n-SSPAC
AS1-n
AS1-n-PAC
AS1-n-SPAC
AS1-n-SSPAC
AS2-n
AS2-n-PAC
AS2-n-SPAC
AS2-n-SSPAC
KS0-n
KS0-n-PAC
KS0-n-SPAC
KS0-n-SSPAC
KS0.1-n
KS0.1-n-PAC
KS0.1-n-SPAC
KS0.1-n-SSPAC
Solid-phase iodine concentration (mg/g)
Liquid-phase iodine concentration (g/L)
10000
1000
100
0.1
1
10

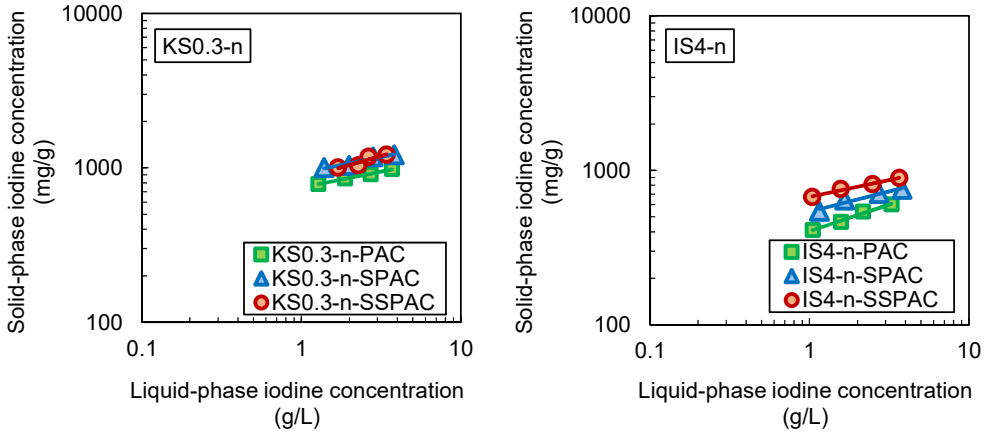
KS0.3-n
KS0.3-n-PAC
KS0.3-n-SPAC
KS0.3-n-SSPAC
IS4-n
IS4-n-PAC
IS4-n-SPAC
IS4-n-SSPAC
Solid-phase iodine concentration (mg/g)
Liquid-phase iodine concentration (g/L)
10000
1000
100
0.1
1
10

(b) (Phenol)

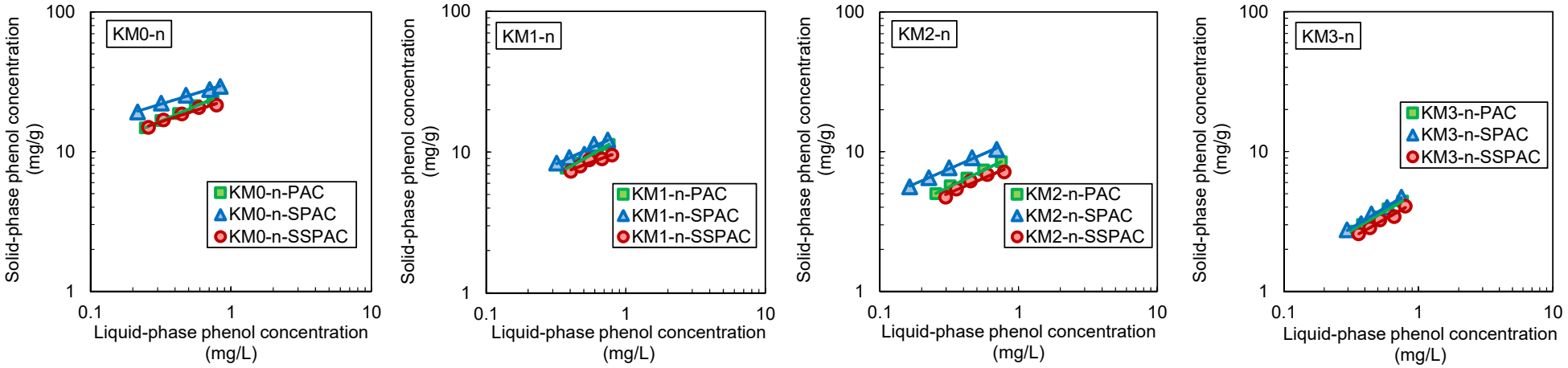
KM0-n
KM0-n-PAC
KM0-n-SPAC
KM0-n-SSPAC
KM1-n
KM1-n-PAC
KM1-n-SPAC
KM1-n-SSPAC
KM2-n
KM2-n-PAC
KM2-n-SPAC
KM2-n-SSPAC
KM3-n
KM3-n-PAC
KM3-n-SPAC
KM3-n-SSPAC
Solid-phase phenol concentration (mg/g)
Liquid-phase phenol concentration (mg/L)
100
10
1
0.1
1
10

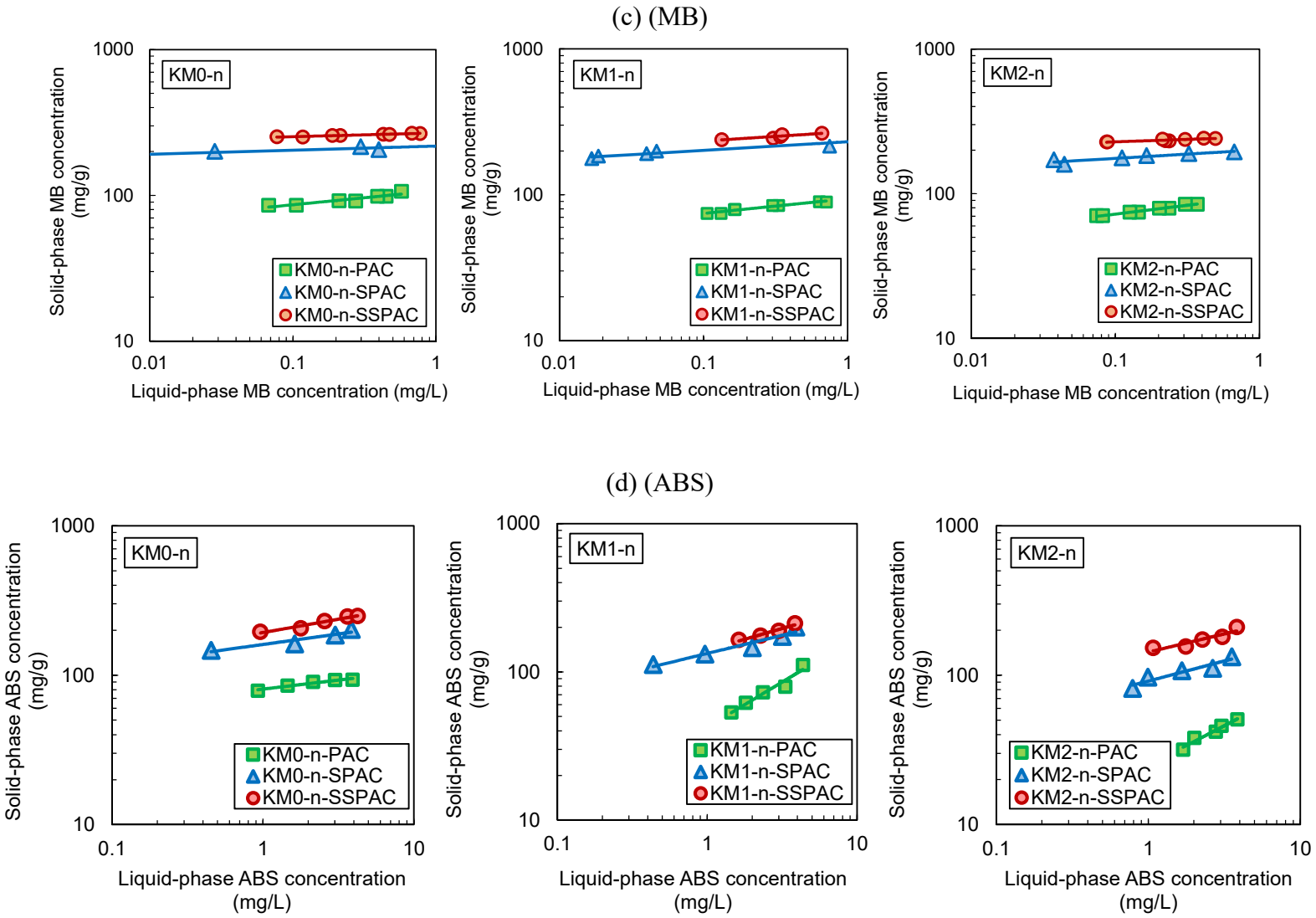

Fig. S10 – Solid-phase vs. liquid-phase concentrations used to determine iodine number, phenol number, MB number, and ABS number.

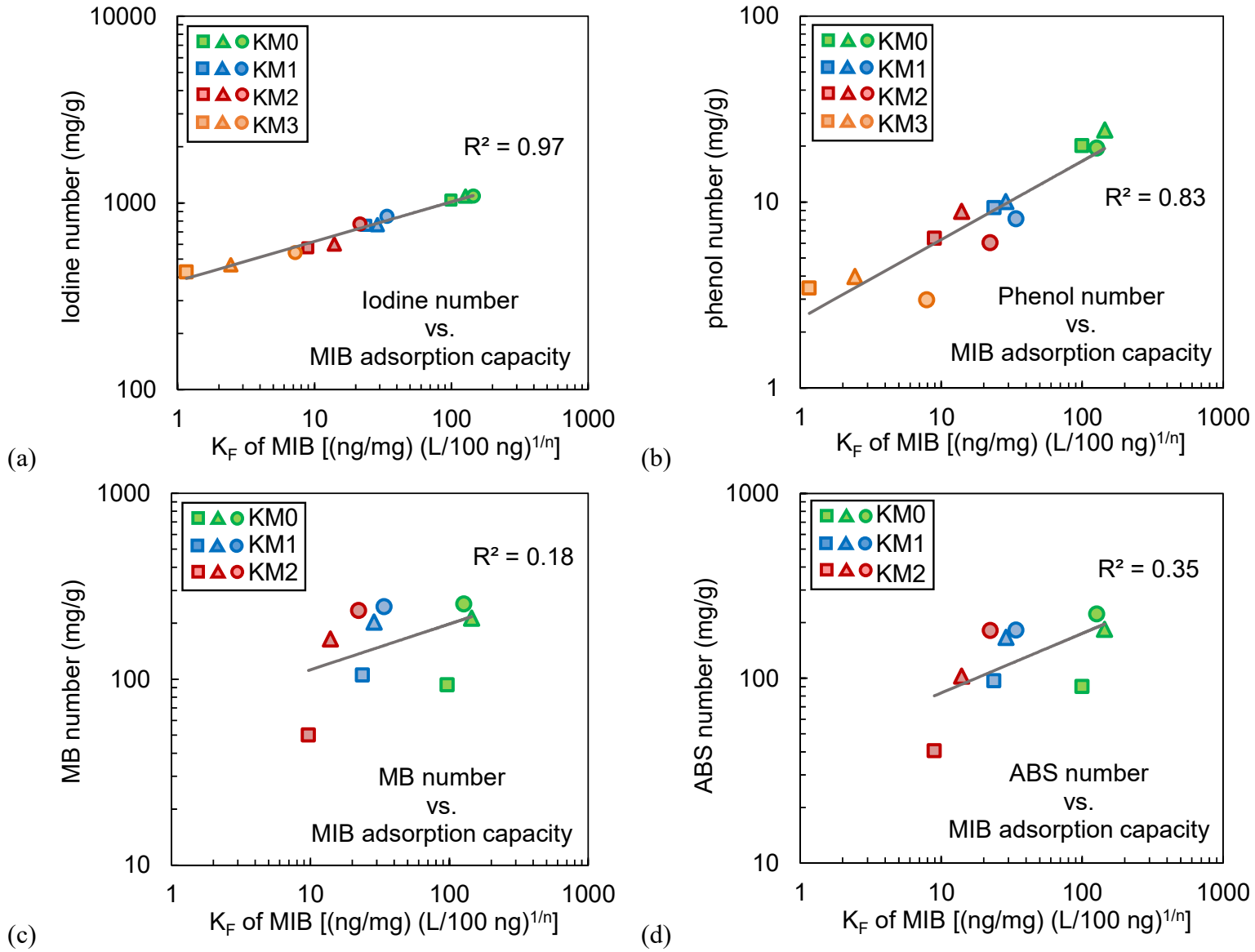

Fig. S11 – Correlation between MIB adsorption capacity and four indices of the KM-series carbon (the squares are PACs, the triangles are SPACs, and the circles are SSPACs).

(a) (phenol with 1-mg/L initial concentration [0.5-day contact time], working solution C [organic-free ionic water])

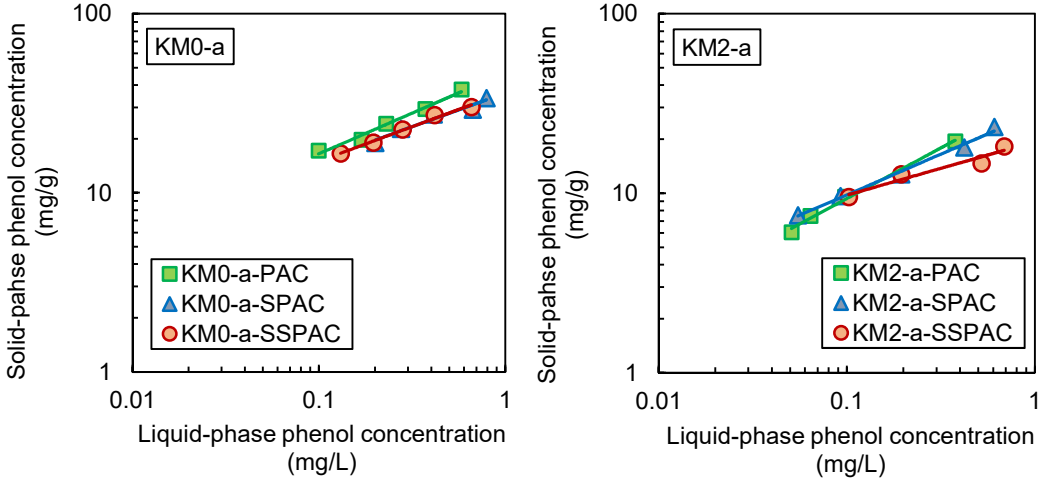

(b) (acetaminophen with 2-mg/L initial concentration [7-day contact time], working solution C [organic-free ionic water])

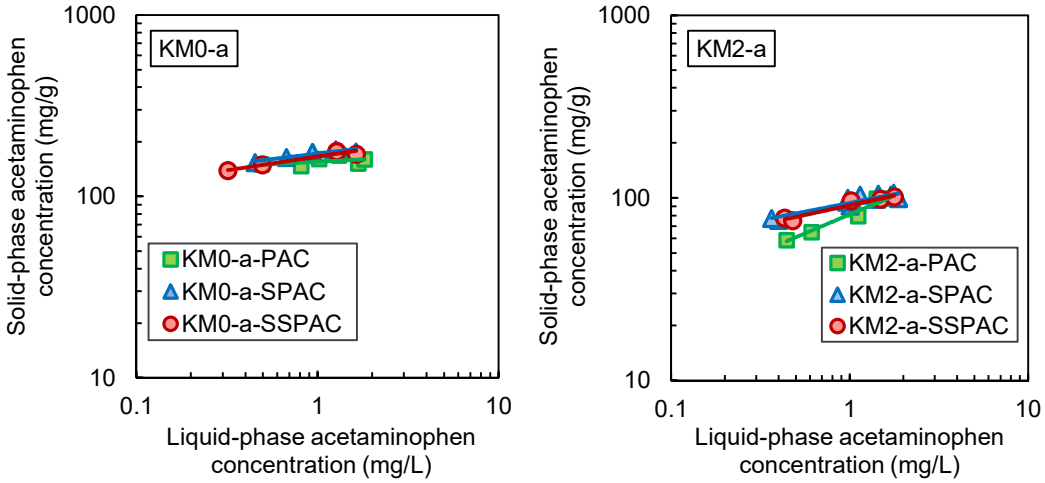

(c) (acetaminophen with 10-µg/L initial concentration [0.5-day contact time], working solution C [organic-free ionic water])

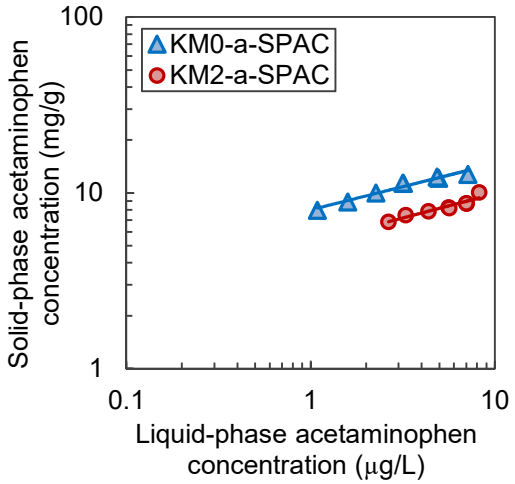

(d) (MIB with 1-µg/L initial concentration [7-day contact time], working solution C [organic-free ionic water])

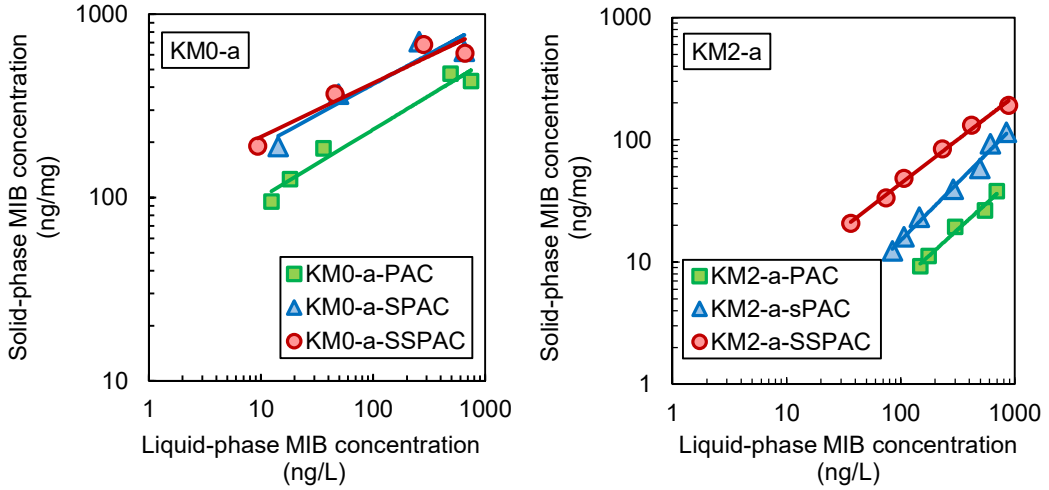

(e) (geosmin with 1-µg/L initial concentration [7-day contact time], working solution C [organic-free ionic water])

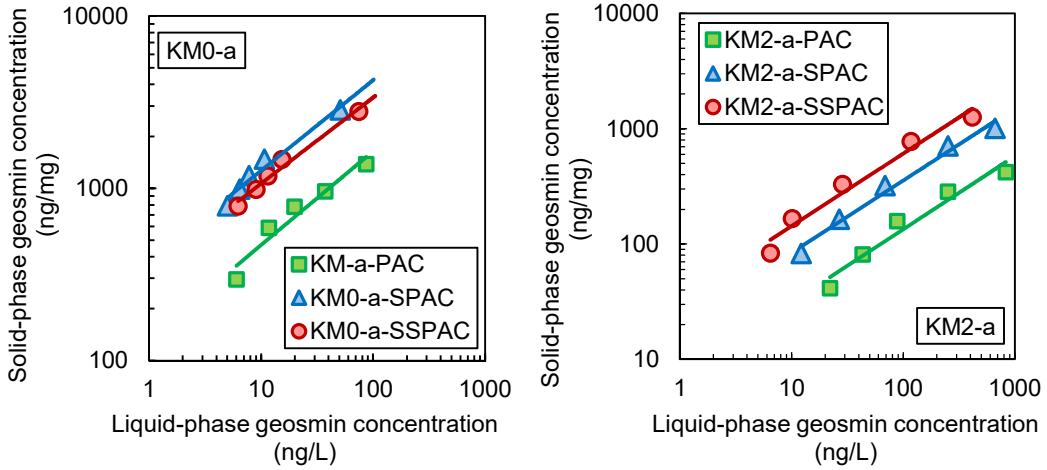

(f) (MB with 0.48-mg/L initial concentration [7-day contact time], working solution D [phosphate buffer water])

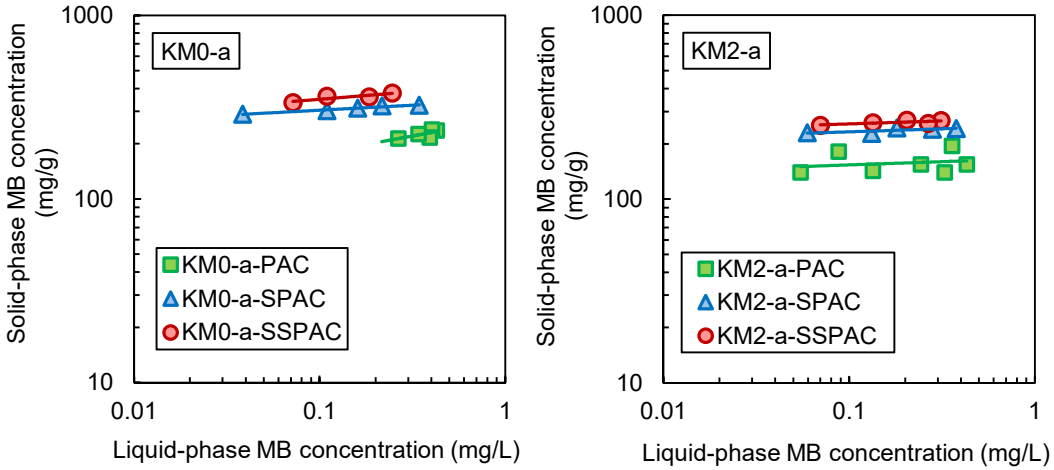

(g) (ABS with 5-mg/L initial concentration [7-day contact time], working solution C [ultrapure water])

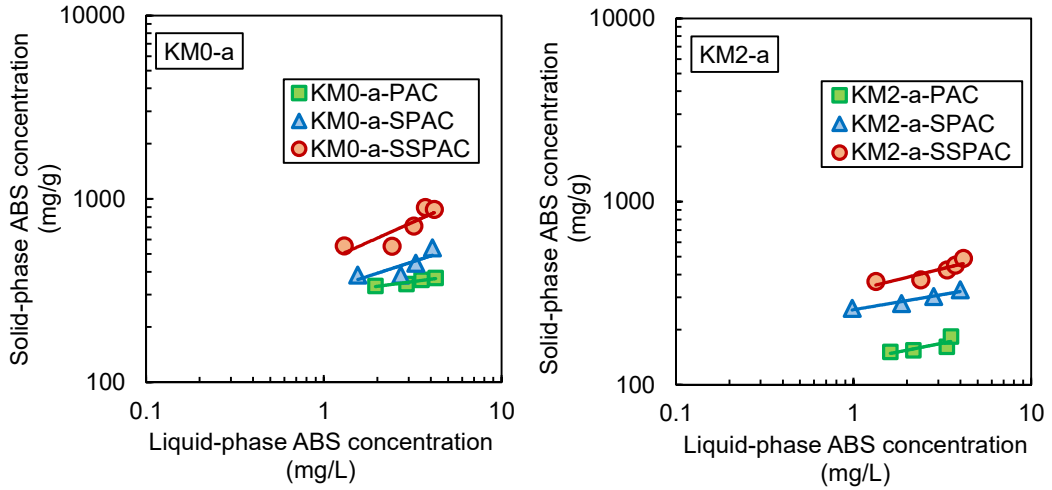

(h) (PSS-210 with 4-mg/L initial concentration [7-day contact time], working solution C [organic-free ionic water])

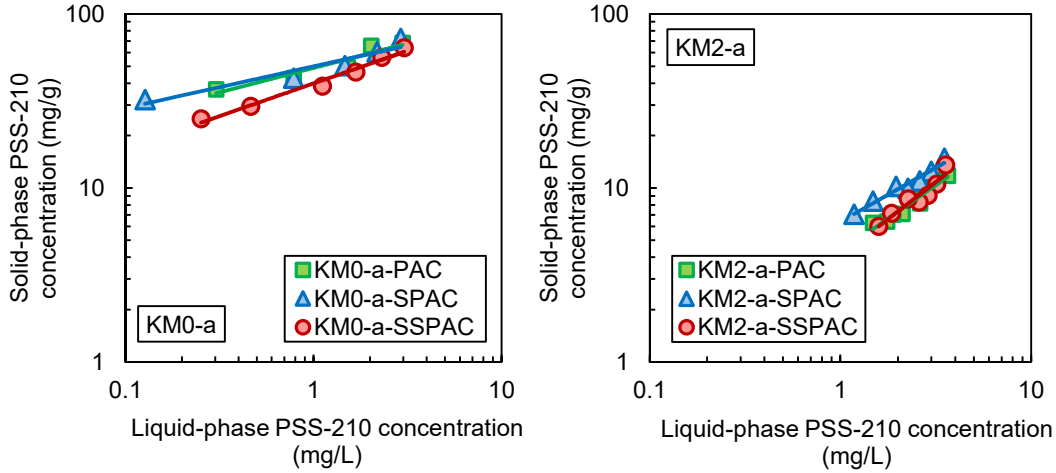

(i) (PSS-6400 with 4-mg/L initial concentration [7-day contact time], working solution C [organic-free ionic water])

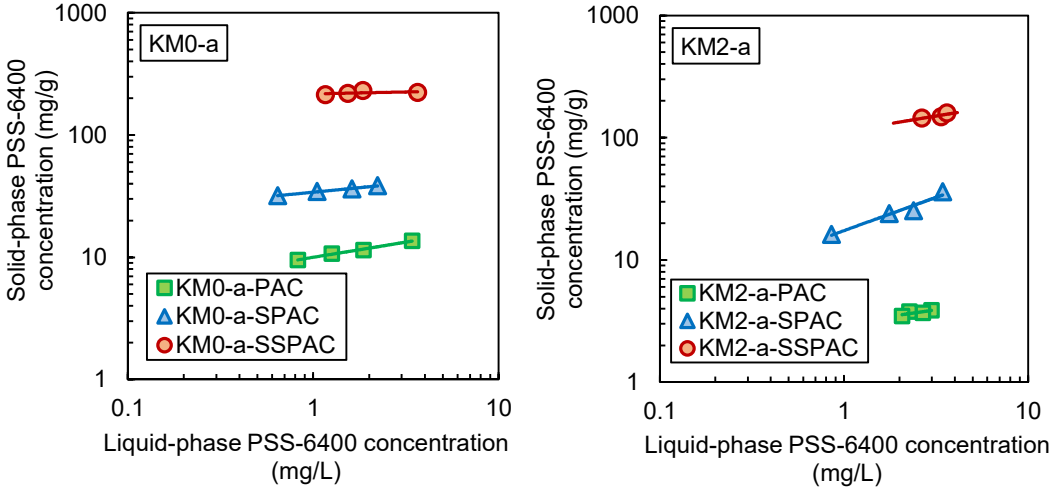

Fig. S12 – Adsorption isotherms of the eight adsorbates.

References

Graham, M.R., Summers, R.S., Simpson, M.R. and MacLeod, B.W., 2000. Modeling equilibrium adsorption of 2-methylisoborneol and geosmin in natural waters. Water Research 34(8), 2291-2300.

JWWA, 2005. Powdered activated carbon for water treatment (K 113:2005-2), Japan Water Works Association, Tokyo, Japan.

Matsui, Y., Nakao, S., Sakamoto, A., Taniguchi, T., Pan, L., Matsushita, T. and Shirasaki, N., 2015. Adsorption capacities of activated carbons for geosmin and 2-methylisoborneol vary with activated carbon particle size: Effects of adsorbent and adsorbate characteristics. Water Research 85, 95-102.

Newcombe, G., Morrison, J. and Hepplewhite, C., 2002. Simultaneous adsorption of MIB and NOM onto activated carbon. I. Characterisation of the system and NOM adsorption. Carbon 40(12), 2135-2146.